A Letter of Intent to PAC48

Sub- and Near-threshold Production of J/ψ Mesons from a Deuterium Target at SoLID

D. Byer, H. Gao[‡], B. Karki, V. Khachatryan, G. Matousek
X. Li, A.P. Smith, E. van Nieuwenhuizen, B. Yu, Z.W. Zhao, J. Zhou
Duke University, Durham, NC 27708, USA

T.-S. Harry Lee
Argonne National Laboratory, Lemont, IL 60439, USA

C. Ayerbe, H. Bhatt, D. Bhetuwal, T. Chetry,

B. Devkota, J. Dunne, D. Dutta, L. El-Fassi, A. Karki

Mississippi State University, Mississippi State, MS 39762, USA

J.P. Chen, T. Liu
Thomas Jefferson National Accelerator Facility, Newport News, VA 23606, USA

X.Z. Bai, J. Boyd, K. Gnanvo, S. Jeffas, S. Jian, N. Liyanage,

J. Matter, H. Nguyen, A. Rathnayake, J. Zhang, X. Zheng
University of Virginia, Charlottesville, VA 22904, USA

[‡]Contact person: `hgao@duke.edu`

Abstract

The production of J/ψ meson near the threshold from the proton has attracted extensive interests in recent years in light of the experimental findings of the hidden charm pentaquark candidates by the LHCb collaboration, and also by its connection to the QCD trace anomaly, predicted to contribute significantly to the mass of the proton. There is also a renewed interest in probing the QCD van der Waals interaction – mediated by multi-gluon exchanges – which is expected to dominate the interaction between two hadrons when they have no common quarks. Such an attractive interaction also leads to the prediction that a bound state between a J/ψ and a light nucleus can exist. Subthreshold production of mesons such as ϕ or J/ψ from a nuclear target is expected to enhance such attractive interaction, and also allow for a direct probe of short range correlations inside a nucleus. Further, through rescattering, the production of J/ψ meson from the deuteron – both below and above the production threshold from a single nucleon (8.2 GeV) – provides an excellent way to extract the $J/\psi - N$ potential, and to compare such information directly from the lattice QCD prediction.

In this letter of intent, we propose to perform measurements of subthreshold and near threshold real photoproduction and low Q^2 electroproduction (quasi-real photoproduction) of J/ψ meson from the deuteron using a 15-cm liquid deuterium target and the proposed SoLID device in Hall A. An electron beam at an incident energy of 8.5 GeV and a beam current of 1.25 μA will be utilized, and the liquid deuterium target will also serve as a photon radiator. The two decay electron and positron from the J/ψ will be detected in coincidence to reconstruct the parent particle, while the recoil proton will also be detected. In the case of electroproduction, the scattered electron is not required for detection to favor the quasi-real photoproduction with low Q^2. Such triple-coincidence measurements are possible thanks to the high luminosity and large acceptance associated with the SoLID device. The proposed experimental configuration will be the same as that of the approved SoLID J/ψ experiment from the proton (E12-12-006). The production cross-section from the proton near the threshold from E12-12-006 will be used as an important input to the theoretical calculation of the subthreshold and near threshold production from the deuteron. The proposed experiment will allow for the extraction of the $J/\psi - N$ potential and to test the lattice QCD prediction, and to probe the short-range correlation inside the deuteron. The total requested beam time is 50 days.

Contents

1 Introduction

The multi-quark state is one of the active frontiers since the establishment of the quark model [1]. Hadrons, as color singlet states, are composite particles made of quarks and gluons held together by strong interactions. Ordinary mesons are described as quark-antiquark states and ordinary baryons are described as three-quark states. Exotic mesons, such as glueballs, tetraquarks, and hybrid mesons, have quantum numbers that are impossible for a quark-antiquark configuration. Similarly, exotic baryons have constituents other than the three-quark configuration. The pentaquark is a type of exotic baryons whose minimum-quark-content is five-quark. The quantum chromodynamics (QCD) is known as the fundamental theory of strong interactions in the framework of the Yang-Mills gauge theory with quarks and gluons as degrees of freedom. It allows the existence of multi-quark states – however, due to the non-perturbative nature of QCD at low energy scales – first principle calculations of hadronic states and properties remain challenging. Hence experimental investigation of multi-quark states is an important approach to understand the dynamics of the strong interaction at the hadronic scale.

The production of J/ψ mesons near the threshold from protons has attracted extensive interests in recent years in light of the experimental findings of the hidden charm pentaquark candidates by the LHCb collaboration. In 2015, LHCb discovered two hidden charm pentaquark candidates, named as $P_c(4380)$ and $P_c(4450)$, in the channel $\Lambda_b \to J/\psi K^- p$ [2], which contains narrow peaks in the $J/\psi p$ invariant mass distribution. In 2019, LHCb followed up with an order of magnitude more data to discover another narrow pentaquark candidate $P_c(4312)^+$ and to confirm that $P_c(4450)^+$ consists of two narrow overlapping peaks, $P_c(4440)^+$ and $P_c(4457)^+$ [3]. The 12-GeV CEABF at Jefferson Lab provides excellent opportunities to study the production of J/ψ mesons near the threshold as demonstrated by the GlueX experiment in Hall D [4]. The GlueX collaboration reported on the measurement of the $\gamma p \to J/\psi p$ cross section for photon energies from 11.8 GeV down to the threshold energy of 8.2 GeV using a tagged photon beam. The results show that the total cross section falls toward the threshold less steeply than expected from two-gluon exchange models [5]. While the LHCb pentaquark candidates P_c^+ in principle could be produced in the s channel of this reaction, the GlueX results provide no evidence for these states. Another Jefferson Lab experiment E12-16-007 [6] took data in Hall C in spring 2019 on photoproduction of J/ψ on the proton from the threshold of 8.2 GeV to energies above the threshold for the production of the $P_c(4450)$ state, and the data from that experiment is currently being analyzed.

Precise information on the cross section of the J/ψ meson from the proton near the threshold has also attracted major experimental and theoretical activities because of its connection to the QCD trace anomaly, which is predicted to contribute significantly to the mass of the proton. The proton, as the bound state of strong interaction, is fundamentally described in terms of quarks and gluons degrees of freedom in QCD. Thus, a partition of the proton mass can be investigated from QCD energy-momentum tensor, which can be uniquely separated into a traceless and a trace parts following the procedure in Refs. [7, 8].

According to the separation of the energy-momentum tensor, one can partition the proton Hamiltonian in terms of the quark energy, gluon energy, quark mass, and the trace anomaly contributions. The parameter b that determines the trace anomaly contribution to the proton mass, which also contributes to the quark mass and quark energy pieces can be extracted via the purely real amplitude of the interaction between heavy quarkonium and light hadron at low energy [9, 10]. The heavy quarkonium, such as J/ψ, is a strongly bound state of two heavy quarks with both the constituents' mass and the binding energy much larger than $\Lambda_{\rm QCD} \sim 340\,{\rm MeV}$ [11], the typical nonperturbative QCD scale. Thus, it can be utilized as a microscopic probe of the structure of light hadrons, such as the proton. The quarkonium-nucleon scattering $J/\psi N \to J/\psi N$ is related to the differential cross section of forward photoproduction $\gamma N \to J/\psi N$ process through the conventional vector meson dominance (VMD) approach [10]. The SoLID spectrometer at Jefferson Lab is designed to operate in a high luminosity environment with large acceptance, and thus presents the unique advantage for such measurements where the cross-section is small and rapidly changing. The approved E12-12-006 experiment with SoLID [12] will measure the exclusive J/ψ electro- and photo-production processes, and extract both the differential and total cross-sections close to the threshold with high precision. The results will shed light on the determination of the b parameter and consequently the trace anomaly part of the proton mass.

There is also a renewed interest in probing the QCD van der Waals interaction – mediated by multi-gluon exchanges – which is expected to dominate the interaction between two hadrons when they have no common quarks. Such an attractive interaction in the case of the $J/\psi - N$ has been confirmed by both the effective field theory method [13–16] and lattice QCD [17]. This van der Waals attractive interaction also leads to the prediction of a bound state between a J/ψ and a light nucleus [18]. Experimental determinations of the $J/\psi - N$ interaction are important not only for investigations of bound J/ψ nuclear states [19], but also important for testing lattice QCD predictions. Wu and Lee [20] studied quasi-free production of J/ψ from the nucleon inside the deuteron near the threshold, and found at forward proton scattering angles and low J/ψ momenta in the center-of-mass frame of the $J/\psi - N$ subsystem, the differential cross section is dominated by the $J/\psi - N$ rescattering. Therefore, carefully designed experiments using a deuterium target will allow for the extraction of the $J/\psi - N$ potential. Both sub- and near-threshold production of J/ψ is advantageous in this case to access low J/ψ momentum, therefore the rescattering region. Previously, "subthreshold" production of ϕ mesons from a deuterium target has been demonstrated by CLAS6 [21], in which the physical threshold of the ϕ meson photo-production from the proton was determined by the detection acceptance of the decay kaon pair. Subthreshold production of J/ψ meson was also attempted previously in Hall C at the 6-GeV CEBAF [22], with no events seen for such production. The null finding is not surprising as sub-threshold cross sections are small, and 5.7 GeV used for the experiment is too far from the threshold of 8.2 GeV. Recently Hatta *et al.* [23] proposed sub-threshold photo-production of J/ψ from nuclear targets as an independent test of the universality of the nucleon-nucleon short range correlation in nuclear scattering processes, and the deuteron is presented as the reference nucleus for such a test.

In this letter of intent (LOI), we propose to perform measurements of sub- and near-threshold photo- and electro-production of J/ψ mesons from the deuteron using a 15-cm liquid deuterium target and the proposed SoLID device in Hall A. An electron beam at an incident energy of 8.5 GeV will be utilized, and the liquid deuterium target will also serve as a photon radiator. For both the electro- and photo-production processes, the recoil proton will be detected in coincidence with the two decay electron and positron from the J/ψ. Such triple-coincidence measurements are possible thanks to the high luminosity and large acceptance associated with the SoLID device. The proposed experimental configuration will be the same as that of the approved SoLID J/ψ experiment from the proton (E12-12-006). The production cross-section from the proton near the threshold from E12-12-006 will also be used as an important input to the theoretical calculation of the sub- and near-threshold J/ψ production from the deuteron. The proposed experiment will allow for the extraction of the $J/\psi - N$ potential and to test the lattice QCD prediction, and to probe the short-range correlation inside the deuteron. The physics motivation of this LOI is complementary to that of the previously conditionally approved Hall C experiment PR12-07-106 [24] and the CLAS12 experiment E12-11-003b [25].

The LOI is organized as follows. We first briefly review theoretical predictions and calculations most relevant to the proposed measurements in Section 2, and then we describe the proposed experimental setup involving the SoLID apparatus, acceptance, triggers, and tracking in Section 3. The backgrounds, projections, and the beam time request are presented in Section 4. A brief summary is drawn in the last section.

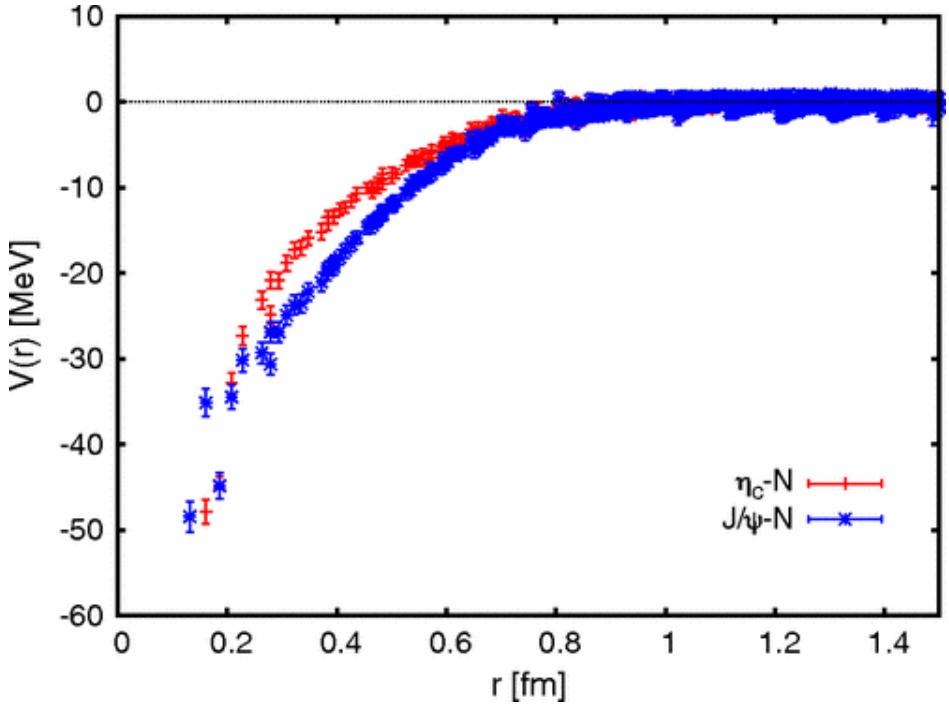

Figure 1: The central and spin-independent part of the J/ψ potential at $M_\pi = 640$ MeV. Also plotted is the $\eta_c - N$ potential for comparison. The figure is from Reference [17].

2 Theoretical Backgrounds and Predictions

The focus of this LOI is on the experimental determination of the $J/\psi - N$ potential from sub- and near-threshold production of the J/ψ meson production from the deuteron and the investigation of the nucleon-nucleon short range correlation (SRC) effect. In this section, we will first review the lattice QCD prediction of the $J/\psi - N$ potential, followed by a recent study on testing the universality of SRC using sub-threshold production of heavy quarkonium. We will then discuss a coupled-channel calculation of J/ψ production from the deuteron near the threshold and how one uses such a process to extract the $J/\psi - N$ interaction. Finally we will describe a calculation of sub-threshold J/ψ photo-production from the deuteron based on a Pomeron-exchange model that this Letter of Intent is based on for calculating the rates.

2.1 Charmonium-nucleon potential from lattice QCD

A non-relativistic Yukawa-type attractive potential, $V_{Q\bar{Q}-N} = -\alpha \frac{e^{-\mu_0 r}}{r}$ is often used to characterise the QCD van der Waals interaction mediated by multi-gluon exchange. However, the strengthens of the $J/\psi - N$ interaction deduced in the literature are different. For example with $\mu_0 = 0.6$ GeV, a $J/\psi - N$ scattering length of -8.83 fm is obtained with $\alpha = 0.6$ [18],

while with $\alpha = 0.06$, it is -0.05 fm [16].

There has been a number of lattice QCD studies of charmonium-nucleon interactions reported in the literature. Yokokawa *et al.* carried out a first lattice QCD study of low-energy charmonium-hadron interaction, and obtained the $J/\psi - N$ ($\eta_c - N$) spin-averaged scattering length of 0.70 ± 0.48 fm (0.70 ± 0.66 fm) [26], which is found to be at least by one order of magnitude larger than the charmonium-pion scattering length. Kawanai and Sasaki [17] reported results on the charmonium-nucleon potential $V_{c\bar{c}-N}$ from quenched lattice QCD for the first time. The result was obtained from calculating the equal-time Bethe-Salpeter amplitude through the effective Schrödinger equation following what was used originally for calculating the $N - N$ potential on the lattice [27]. In the quenched lattice simulations carried out in [17], two different lattice sizes were used, $L^3 \times T = 32^3 \times 48$ and $16^3 \times 48$ with a lattice cutoff of $a^{-1} \approx 2.1$ GeV. The main results are obtained from the data taken with larger lattice ($La \approx 3.0$ fm), while supplementary data with smaller lattice ($La \approx 1.5$ fm) are used for studying finite-size effects. In this study, the pion mass has been varied from 870 MeV down to 640 MeV. There is no significant finite-size effect has been seen, nor a large quark mass dependence is observed in [17]. The authors of [17] found that the potential $V_{c\bar{c}-N}$ for either η_c or J/ψ states to be weakly attractive at short distances – with J/ψ somewhat more attractive – and exponentially screened at large distances. Fig. 1 shows the lattice result on the central and spin-independent part of the J/ψ potential together with the lattice prediction for the $\eta_c - N$ potential.

The authors of [17] fitted their lattice data to the Yukawa form $-\alpha e^{-\mu_0 r}/r$ and obtained $\alpha \sim 0.1$ and $\mu_0 \sim 0.6$ GeV. These fitted values should be compared with $\alpha = 0.6$, and $\mu_0 = 0.6$ GeV from [18], which are barely fixed by a Pomeron exchange model. So the fitted α value is about six times weaker than that from the phenomenology. However, the authors of [17] also pointed out in their paper that "we speculate that the $c\bar{c} - N$ potential from dynamical simulations would become more strongly attractive in the vicinity of the physical point, where the size of the nucleon is much larger than at the quark mass simulated in this study." Recently a Hamiltonian model [28] was developed using the $J/\psi - N$ potential extracted from the lattice QCD calculation [17] to calculate the J/ψ photoproduction cross section from the proton. The predicted total cross sections are consistent with the most recent results [4] from the GlueX experiment at Jefferson Lab. The experimental extraction of the $J/\psi - N$ potential would allow one to test such a lattice QCD prediction as well as future dynamic lattice QCD simulations.

2.2 Sub-threshold J/ψ production and short range correlations

The nucleon-nucleon short-range correlation (SRC) inside a nucleus refers to the situation when a pair of nucleons (mostly a proton and a neutron) are close together in configuration space – while in momentum space – the pair has a large relative momentum but with a small total momentum. The nucleon-nucleon SRC as an important aspect of the nuclear

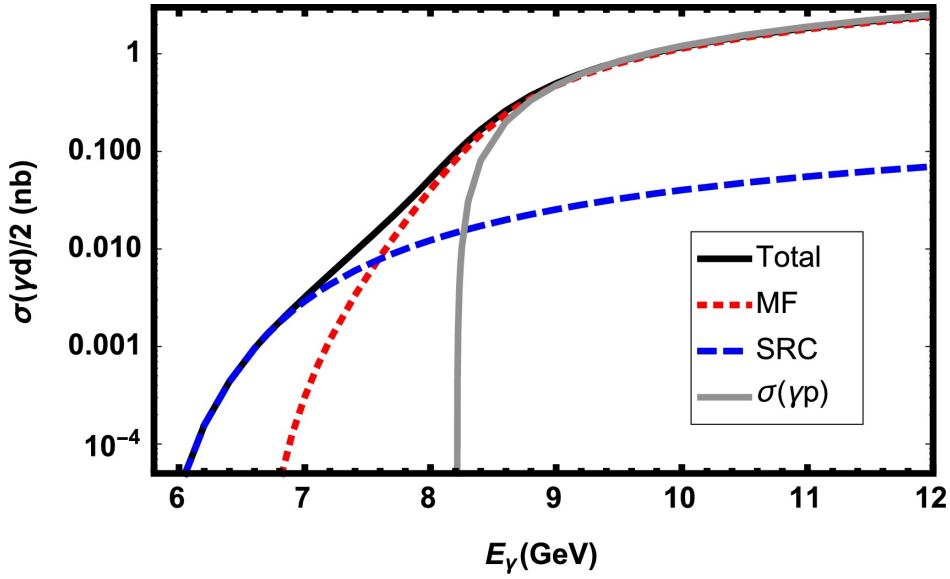

Figure 2: The sub-threshold photo-production cross sections per nucleon as a function of photon energy from the deuteron in the target rest frame. The near threshold production cross section from the proton is also plotted (grey solid curve) for reference. The result from the mean field (MF) is shown as the red dashed curve, SRC is shown as the blue dashed curve, and the total is the black solid curve. The figure is from Reference [23].

structure, has attracted even greater interests in recent years [29–34] because it may hold the clue to understand the EMC effect observed in nuclear structure function measurements as inspired by recent SRC experiments at Jefferson Lab [35–45]. Experimentally it is important to demonstrate the universality of nucleon-nucleon SRC which is necessary if SRC is the underlying reason behind the observed EMC effect. Recently Hatta, Strikman, Xu and Yuan [23] proposed that J/ψ and Υ sub-threshold production in photo-nuclear processes – where the threshold refers to the minimum photon energy required to produce a J/ψ or Υ meson on the proton – can provide such an independent test of the universality of the nucleon-nucleon SRC in nuclear scattering processes.

The deuteron is an excellent choice for such a study as it is the simplest nuclear system with one pair of a proton and a neutron. Sub-threshold production of J/ψ on the nucleon inside the deuteron selects high Fermi-momentum nucleon, i.e. large relative momentum nucleon-pair but with zero total momentum as the deuteron is at rest in the lab frame, therefore the SRC region. The deuteron also provides an excellent reference for sub-threshold production from other nuclei in the context of testing the universality of SRC. Fig. 2 shows the results [23] on the subthreshold photo-production of the J/ψ meson from the deuteron per nucleon as a function of the incident photon energy. Also plotted is the corresponding cross section from the proton as a reference. One can see that the SRC dominates the subthreshold production cross section at photon energies below 7.5 GeV, above which the mean field contribution becomes important and dominant.

To test the universality of the SRC, Hatta *et al.* [23] calculated the ratio of the sub-threshold production cross section of J/ψ per nucleon from ^{12}C to that of the deuteron as a function of the incident photon energy, and the results are shown in Fig. 3. The plateau region corresponding to photon energies between 6.5 to 7.4 GeV is suggested as the place to observe the universality of the SRC, which is also the region that the SRC contribution dominates the sub-threshold production cross section. However, it is clear from these figures that the aforementioned region is extremely challenging to access due to the smallness of the cross sections being so far away from the threshold. Although the total cross section from the deuteron for the same subthreshold energy is smaller than that of the ^{12}C nuclear target, being the simplest nucleus in nature allows the technique of using untagged Bremstrahlung photons to achieve a significantly higher photon flux. Therefore, this letter of intent focuses on subthreshold production of J/ψ from the deuteron as it probes the SRC region and also serves as an important reference for the investigation of the universality of the SRC effect. In particular, the data will provide strong constraints on determining the short range part of nucleon-nucleon potential which is crucial in predicting SRC for heavy nuclei. With the success of such a first study of sub-threshold production of J/ψ from the deuteron, we will be interested in pursuing future studies of such production from helium and carbon nuclear targets. As we discussed before, we propose to carry out near threshold production of J/ψ mesons from the deuteron in this LOI. This proposed experiment will also provide a unique way to probe the $J/\psi - N$ potential presented in the previous section, which we will discuss next.

2.3 Coupled-channel calculation of J/ψ production from the deuteron

Photoproduction of the J/ψ from the deuteron near the production threshold (of production from the proton) has been proposed [20] as an effective way to experimentally determining the $J/\psi - N$ potential. The reaction mechanisms including plane-wave impulse approximation, NN rescattering and $J/\psi N$ rescattering are shown in Fig. 4. In the rescattering cases, a J/ψ meson is produced from a nucleon inside the deuteron followed by rescattering of the recoil nucleon, or the produced J/ψ from the spectator nucleon. Wu and Lee [20] calculated the 5-fold differential cross sections for J/ψ production from the deuteron at the incident photon energy that is 100 MeV above the production threshold on the proton to investigate the kinematic region where the reaction is sensitive to the $J/\psi - N$ potential. Their calculation is based on a coupled-channel model with πN, ρN, and $J/\psi N$ channels developed to predict the $\pi + N \to J/\psi + N$ cross sections. In the calculation, the $J/\psi - N$ interaction based on forms from effective field theory approach and lattice QCD are parameterized and used. The other interactions in the model are constrained by the decay width of $J/\psi \to \rho + \pi$ and the total cross section data of πN reactions. The calculated meson-baryon amplitudes are then used to calculate the J/ψ production from the deuteron. Fig. 5 shows the calculated differential cross sections as a function of the J/ψ momentum magnitude in the center of mass frame of the $J/\psi - N$ subsystem for the three separate contributions from

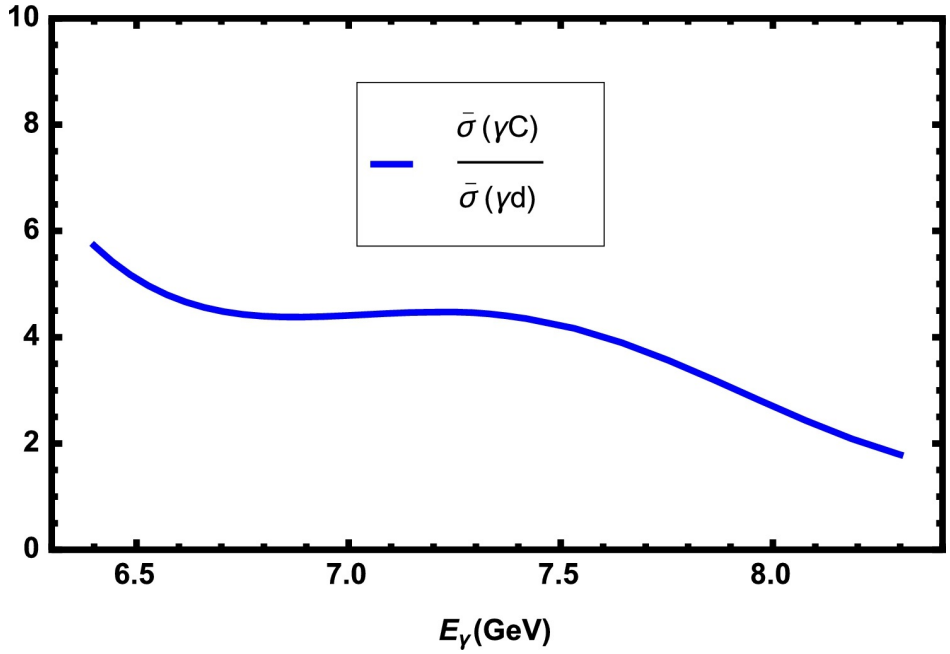

Figure 3: The sub-threshold photo-production cross sections per nucleon as a function of photon energy from the deuteron in the target rest frame. The near threshold production cross section from the proton is also plotted (grey solid curve) for reference. The result from the mean field (MF) is shown as the red dashed curve, SRC is shown as the blue dashed curve, and the total is the black solid curve. The figure is from Reference [23].

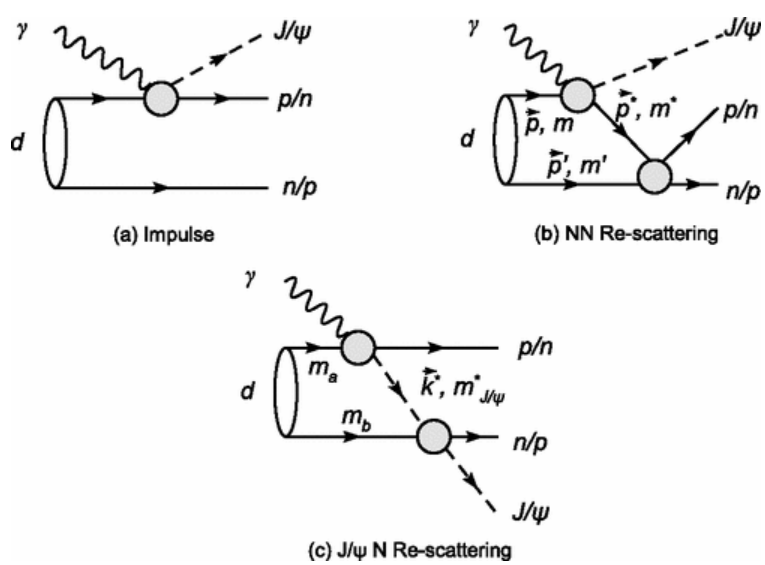

Figure 4: The reaction mechanisms graphically represented for the photo-production of the J/ψ meson on the deuteron: (a) impulse contribution; (b) NN rescattering; (c) $J/\psi - N$ rescattering. The figure is from Reference [20].

impulse, NN rescattering, and $J/\psi - N$ rescattering. The total corresponds to the coherent sum of all the amplitudes. The proton angles shown in both panels of Fig. 5 are with respect to the incident photon momentum and in the rest frame of the target deuteron. These results are obtained with the $J/\psi - N$ potential taking the Yukawa form of $V_{J/\psi-N} = -\alpha \frac{e^{-\mu_0 r}}{r}$, where $\alpha = 0.2$, $\mu_0 = 0.6$ GeV. One sees that at low J/ψ momentum values, the reaction is dominated by the rescattering contribution of the J/ψ from the spectator nucleon with the proton at zero degree, therefore sensitive to the $J/\psi - N$ potential. The sensitivity is demonstrated by Fig. 6 where the α parameter in the potential is chosen for three different values: 0.2, 0.09 and 0.06, while $\mu_0 = 0.6$ GeV, and the proton angle is at zero degree. When the proton angle is at 180°, the production is dominated by the impulse diagram, and as such insensitive to the $J/\psi - N$ interaction. Subthreshold production from the deuteron target is advantageous to select kinematics corresponding to lower J/ψ momentum in the center of mass frame of the $J/\psi - N$ subsystem, i.e. more sensitive to the $J/\psi - N$ potential, though the cross section would be smaller. So in this LOI, we propose to carry out both the sub- and the near-threshold J/Ψ electro- and photo-production from the deuteron to maximize the experimental sensitivity to the $J/\Psi - N$ potential. Such coupled channel calculations specifically for the proposed sub- and near-threshold production of J/ψ will be carried out in the future in developing a full proposal to show the quantitative connection and sensitivity between the proposed measurements and the input $J/\psi - N$ interaction, therefore to allow for an extraction of this potential, and the test of lattice predictions.

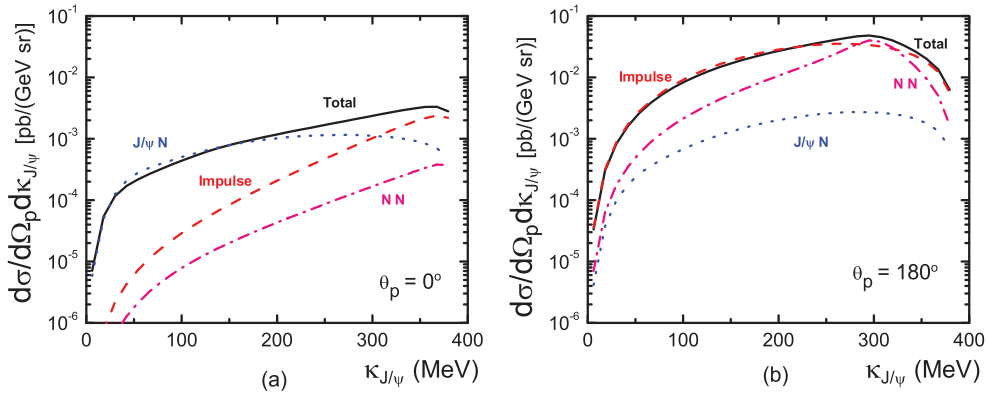

Figure 5: The three-fold differential cross section as a function of the J/ψ momentum in the center of mass frame of the J/ψ and the recoil nucleon inside the deuteron. The blue dotted line corresponds to contribution from the $J/\psi - N$ rescattering, the red dashed curve is for the impulse contribution, the magenta dash-dotted line is from the NN rescattering, and the black solid line is the total. The left panel is for the 0° proton angle, and the right panel is for 180°, where the proton angle is defined with respect to the incoming photon momentum in the rest frame of the deuteron. The figure is from Reference [20].

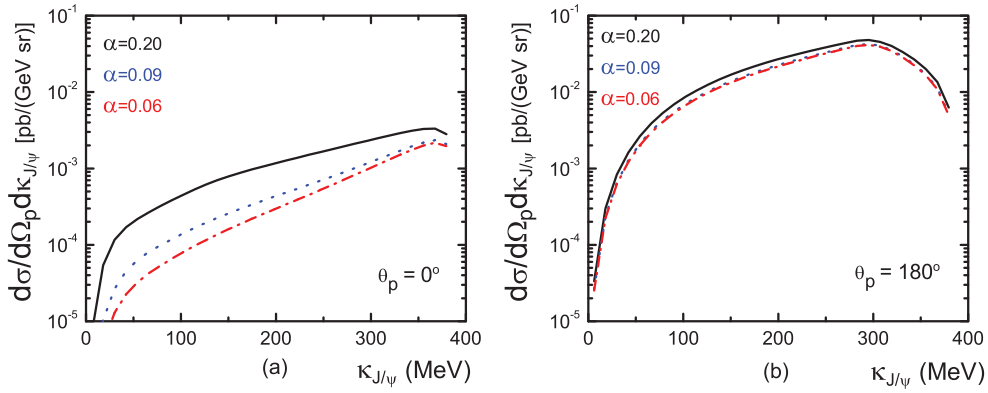

Figure 6: The three-fold differential cross section as a function of the J/ψ momentum in the center of mass frame of the J/ψ and the recoil nucleon inside the deuteron. The three lines correspond to three different values of α (see text). The left panel is for the 0° proton angle, and the right panel is for 180°, where the proton angle is defined with respect to the incoming photon momentum in the rest frame of the deuteron. The figure is from Reference [20].

2.4 Calculation of J/ψ photo-production from the deuteron

In this section, we present results from Harry Lee on the sub-and near-threshold J/ψ production from the deuteron calculated specifically for this letter of intent. The calculations have been performed by using the formulation developed in [20]. For demonstrating the SRC effects and examining the feasibility of the proposed measurements, it is sufficient to only consider the impulse term in Fig. 4a, which gives [20] for the most part the largest contribution to the cross sections. The five-fold differential cross sections of the $\gamma(q)+d(P) \rightarrow J/\psi(k) + N(p') + X_{(A-1)}(P_0)$ reaction in the Laboratory system $P = (M_A, \vec{P} = 0)$ can be written as

$$\frac{d\sigma}{dk\, d\Omega_k\, d\Omega_{p'}} = (2\pi)^4 \frac{k^2 p'^2 E_N(\vec{t}-\vec{p}\,') E_N(\vec{p}\,')}{||\vec{p}\,'|E_N(\vec{t}-\vec{p}\,') + E_N(\vec{p}\,')(|\vec{p}\,'| - \vec{t}\cdot\vec{p}\,'/|\vec{p}\,')|} \times \frac{1}{4} \sum_{\lambda_V, m'_s, \lambda, m_s} [A\rho(\vec{p}\,' - \vec{t}, m_s)]| < k\lambda_V; p'm'_s|T_{\mathbb{P}}|q\lambda_\gamma, pm_s > |^2] \,. \quad (1)$$

where $A = 2$, $\vec{t} = \vec{q} - \vec{k}$, the initial nucleon momentum is determined by $\vec{p} = \vec{p}\,' - \vec{t}$, λ and λ_V are the helicities of the initial photon and final J/ψ, respectively, m_s and m'_s are the z-components of the nucleon spin. The Pomeron-exchange amplitudes $T_{\mathbb{P}}$ are from using the parameters of [20] with the refinements explained in [28]. While this model, as well as other two-gluon and three-gluon exchange models [5], is phenomenological, it is sufficient for our purposes because it is obtained by reproducing the available total cross section data up to invariant mass $W = 300$ GeV. A more fundamental QCD model based on $q\bar{q}$-loop, as explored in Ref.[46, 47], is unfortunately not available to us at the present time. There exists no LQCD effort to calculate J/ψ photoproduction amplitudes.

The nucleon momentum distribution of the deuteron in Eq.(1) is defined by $\rho(\vec{p}, \frac{1}{2}) = \rho(\vec{p}, -\frac{1}{2}) = \frac{1}{2}\rho(p)$, and $\int d\vec{p}\rho(\vec{p}) = 1$. In this calculation, we use $\rho(p)$ from two different nucleon-nucleon potentials and they are the Argonne V18 (AV18) [48] and the nv2IIa potential describing local nucleon-nucleon and three-nucleon interactions based on chiral effective field theory [49]. Details about these two potentials can be found on the webpage of the Argonne Nuclear Theory Group.

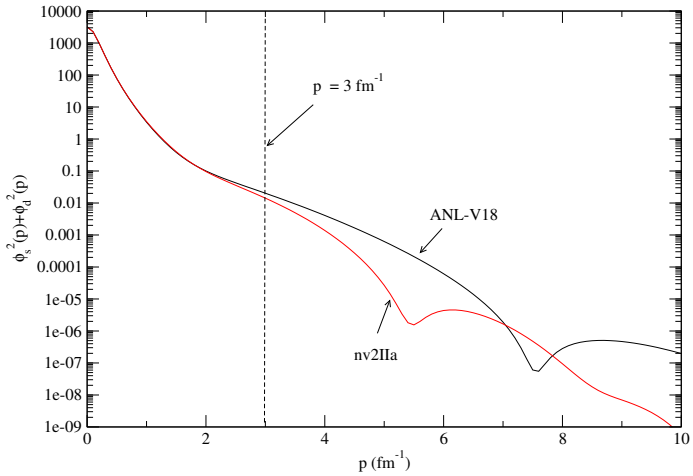

Figure 7: The nucleon momentum distribution in ^{2}H calculated from two nucleon-nucleon potentials. The black curve is from the AV18 and the red curve is from the nv2IIa.

Fig. 7 shows the nucleon momentum distribution in ^{2}H calculated from these two nucleon-nucleon potentials. Below a Fermi momentum less than 3 fm^{-1}, the difference between the two distributions is negligible. However, at larger Fermi momenta, where the SRC effect is important, the AV18 predicts larger SRC effects. Fig. 8 shows the total inclusive photo-production cross section of J/ψ from the deuteron as a function of the incident photon energy based on the AV18 potential. The black curve corresponds to the initial nucleon momentum less than 2 GeV, while the red curve is for less than 0.3 GeV. It is easy to see that larger initial nucleon momentum, i.e. short-range correlation region, gives larger cross section in the sub-threshold region as expected. Fig. 9 shows the calculated total inclusive J/ψ photo-production cross section from the deuteron as a function of the incident photon energy from below the threshold to above. The results from AV18 and nv2IIa are shown in black and red, respectively, and the difference between the two disappears once the energy is above the threshold (8.2 GeV) from the proton. These results indicate that the AV18 provides more SRC effect compared to that of nv2IIa, which is consistent from what we learned in Fig. 7. Sub-threshold production of the J/ψ meson indeed provides a sensitive way to probe the nucleon-nucleon SRC. Fig. 10 shows the sub-threshold inclusive differential cross section from the deuteron as a function of the J/ψ angle in the lab frame at an incident photon energy of 7.2 GeV with the initial nucleon momentum below 2 GeV (black curve) and below 0.3 GeV (red curve). These results are obtained with the AV18 potential. The five-fold differential cross section results obtained with the AV18 potential have been

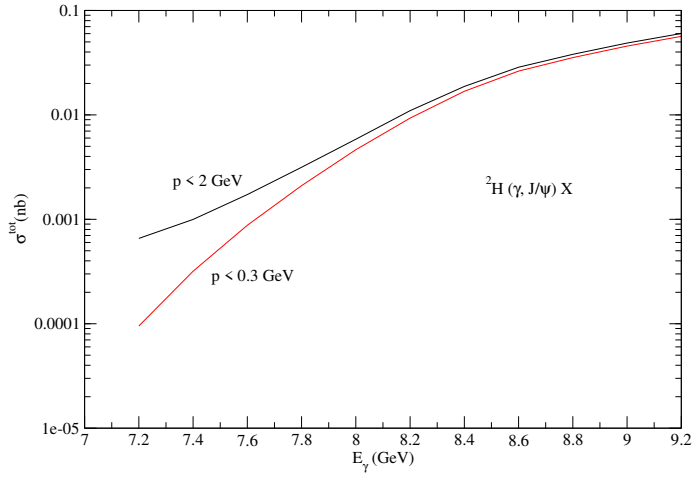

Figure 8: The total inclusive J/ψ photo-production cross section from the deuteron as a function of the incident photon energy from 7.2 GeV to above 9 GeV. The result is from the Argonne V18 potential. The black curve is for the initial nucleon momentum less than 2 GeV, while the red curve is for less than 0.3 GeV.

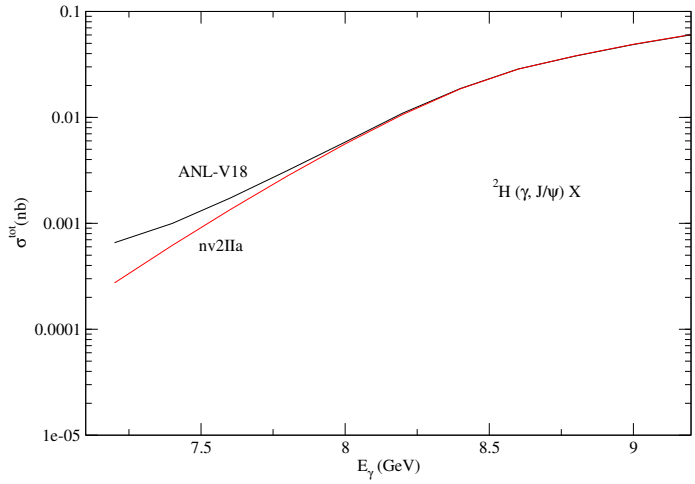

Figure 9: The total inclusive J/ψ photo-production cross section from the deuteron as a function of the incident photon energy from 7.2 GeV to above 9 GeV. The result from the Argonne V18 potential is shown as the black curve, and the result from the nv2IIa is shown as the red curve.

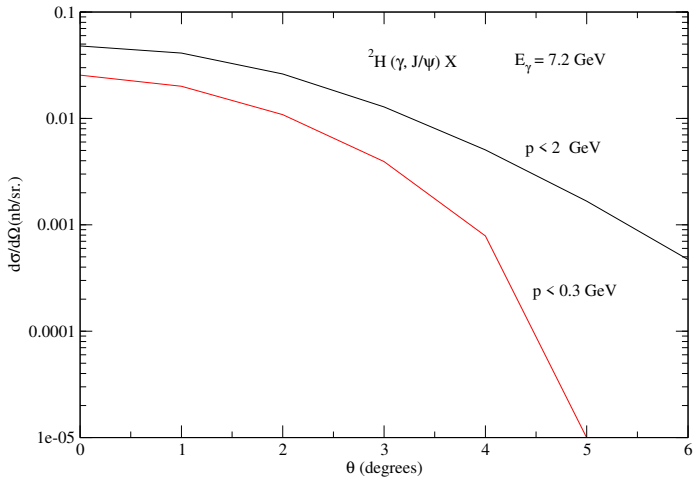

Figure 10: The differential inclusive J/ψ photo-production cross section from the deuteron as a function of the J/ψ angle in the lab frame at an incident photon energy of 7.2 GeV (sub-threshold). The result is from the AV18 potential.

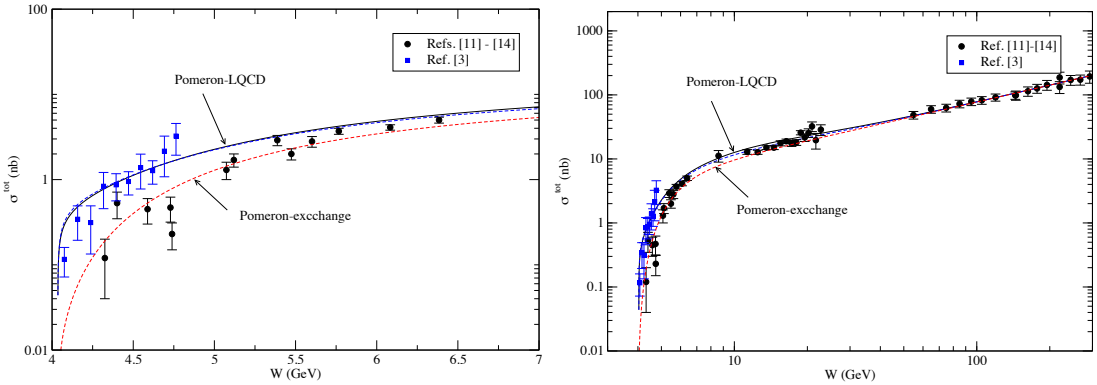

Figure 11: Comparison of the total J/ψ photoproduction cross sections calculated form the Pomeron-LQCD model and the Pomeron-exchange model. The blue points are from recent JLab Hall D experiment [4] and the black ones are old experimental data from Refs. [50–53]. This figure is from reference [28].

used in Section 4.1 to calculate the signal rates for the proposed experiment. The most recent Hamiltonian model based on the vector meson dominance assumption [28] has been extended to include the two-gluon exchange amplitude modeled by Donnachie and Lanshoff within Regge Phenomenology [54]. This results in the Pomeron-LQCD model, which leads to a prediction of near threshold total photoproduction cross section of J/ψ from the nucleon that is more than one order of magnitude larger compared to results based on the Pomeron-exchange amplitude, as shown in Fig. 11, and reproduces the recent JLab Hall D data [4]. Calculations for the proposed measurements using this Pomeron-LQCD model will become available and be used in developing a full proposal. If the JLab Hall D data are comfirmed, we will use the newly developed Pomeron-LQCD model [28], which fits the JLab data as shown in Fig. 11. Our projected rates will be increased drastically.

3 Experimental Setup

We propose to measure the J/ψ sub- and near-threshhold production cross sections on a liquid deuterium target by using the Solenoidal Large Intensity Device (SoLID), a major new detector proposed for Hall A combining large acceptance and high luminosity in the JLab 12-GeV era. The A^- rated experiment E12-12-006 will measure the cross section from J/ψ electro- and photo-production near production threshold on a liquid hydrogen target using SoLID [12]. The experiment has been approved for 60 days including 50 days of production running and 10 days for detector study.

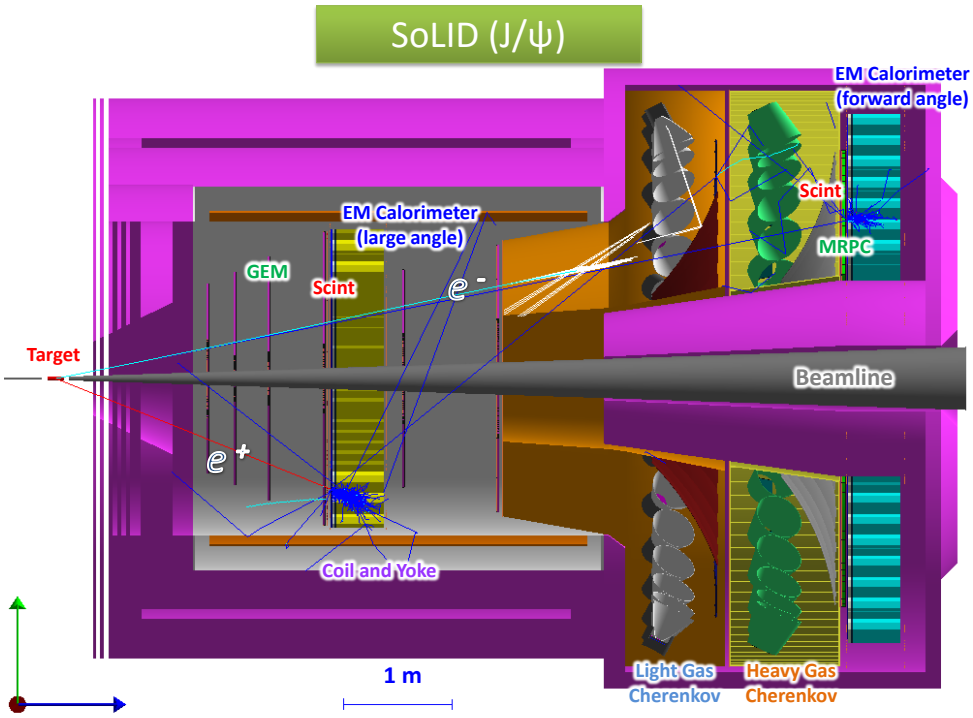

Figure 12: The SoLID J/ψ experimental layout.

Our proposed experiment will use the same SoLID setup of E12-12-006, except we will fill the 15 cm long target cell with liquid deuterium instead of hydrogen. The experience learned from E12-12-006 will be very useful for this experiment and we can save time on detector studies. The layout of the SoLID J/ψ setup is shown in Fig. 12. With custom designed high rate and high radiation tolerant detectors, the SoLID J/ψ setup can carry out experiments using high intensity electron beams incident on a cryogenic target in an open geometry with full azimuthal angular coverage. There are two groups of sub-detectors. The forward angle detector group covers a polar angular range from 8° to 18° and consists of several planes of Gas Electron Multipliers (GEM) for tracking, a light gas Cherenkov (LGC) for e/π

separation, a heavy gas Cherenkov (HGC) for π/K separation, a Multi-gap Resistive Plate Chamber (MRPC) for time-of-flight, a Scintillator Pad (SPD) for photon rejection and a Forward Angle Electromagnetic Calorimeter (FAEC). The large angle detector group covers a polar angular range from 18° to 28° and consists of several planes of GEM for tracking, a SPD and a Large Angle Electromagnetic Calorimeter (LAEC). Electrons, positrons and protons will be detected and identified by measuring their momenta, time-of-flight, photons produced in the threshold Cherenkov detectors, and energy losses in the calorimeters. A single particle geometrical acceptance is shown in Fig. 13 with the target center located at 315 cm upstream from the solenoid coil center. Limited by time-of-flight resolutions, proton identification is good up to momentum 4.5 GeV in the forward angle region and up to 2 GeV in the large angle region.

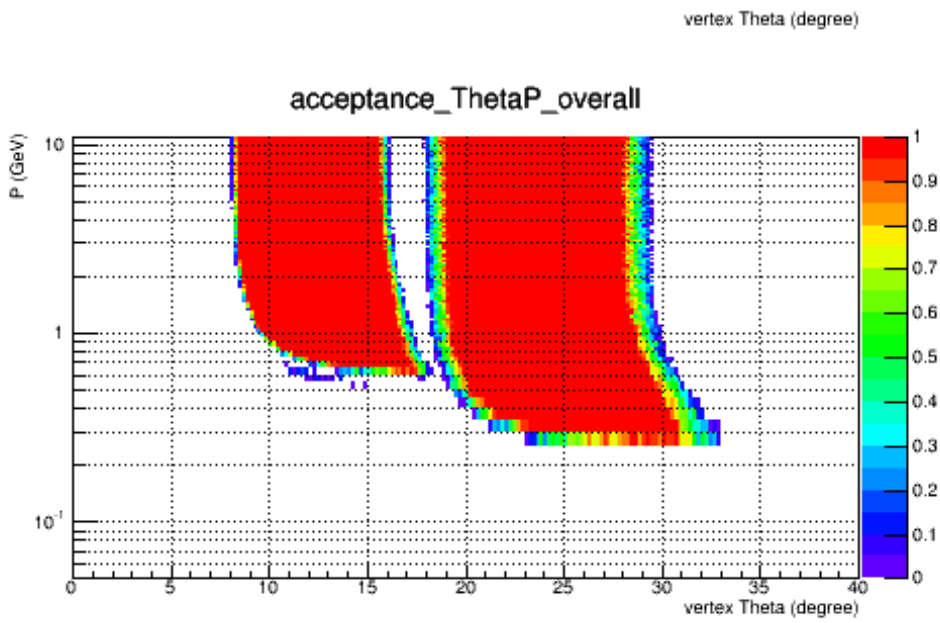

Figure 13: The acceptance of a single particle in SoLID J/ψ setup.

The track resolution of the SoLID J/ψ setup is important in J/ψ identification and rejecting different backgrounds. The expected resolution has been studied using Kalman Filter (KF)-based track finding and track fitting algorithm with digitized GEM simulation data. Fig. 14 shows the expected momentum, angular and vertex z resolution for different polar angles and momentum ranges. Both energy loss in materials (except GEM frame and dead area) and background effects are included. We add an additional safety factor of 1.5 for our study of both the J/ψ signal and background rejection in the following sections.

Because the subthreshhold production is a rare process with small cross sections, we would include both quasi-real photoproduction (low Q^2 electroproduction) and real photoproduction to maximize event counts. As protons detected have momentum > 0.2 GeV

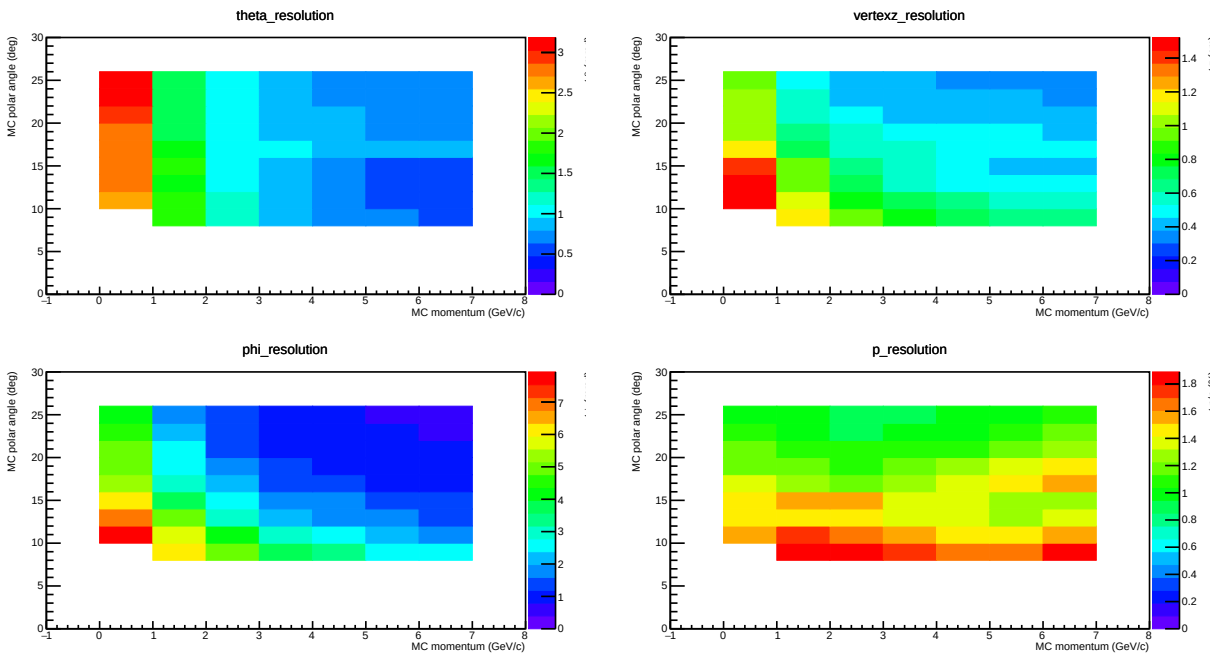

Figure 14: electron and positron track resolutions by track fitting studies with energy loss in materials. Their units are theta(mrad), phi(mrad), vertex z(cm), $\delta_p/p(\%)$. The coordinate system is defined in the lab frame with beam line as the z-axis.

and there is no neutron detection in SoLID, we do not consider the production of J/ψ from the neutron inside a deuteron in this experiment. We will require 3-fold coincident detection of J/ψ decay pairs of electrons and positrons as well as recoil protons, but not the scattered electrons in the case of electroproduction. Thus reactions of interest are $e^- + \text{“}p\text{”} \rightarrow (e^{-'}) + J/\psi + p \rightarrow (e^{-'}) + e^+ + e^- + p$ and $\gamma + \text{“}p\text{”} \rightarrow J/\psi + p \rightarrow e^- + e^+ + p$ where J/ψ is detected through its decay into a lepton pair (e^+, e^-) with a branching ratio of 5.94% and “p” stands for the proton inside the deuteron.

We propose to use a 8.5-GeV electron beam, which is 300 MeV above the threshold energy of J/ψ production on a free proton. The electron beam will induce electroproduction on the target directly and the events detected will be dominated by those from quasi-real photons with relatively larger cross sections. The 15-cm liquid deuterium target also serves as a 2% radiator with which the electron beam will generate bremsstrahlung photons leading to photoproduction events from the rest of the target. In our proposed experiment, we need to know the photon energy to make sure that we separate the J/ψ mesons detected from sub-threshold production, and from above. The quasi-real or real photon energy can be reconstructed from the detected three final state particles by Equation 2.

$$E_\gamma = \frac{M_n^2 + (\overrightarrow{P}_{J/\psi} + \overrightarrow{P}_p)^2 - (E_{J/\psi} + E_p - M_d)^2}{2(P^z_{J/\psi} + P^z_p + M_d - E_{J/\psi} - E_p)}, \tag{2}$$

where we take the incident beam momentum direction to be the z axis, $P^z_{J/\psi}$ and P^z_p are the z component of the J/ψ and recoil proton momentum, correspondingly. This allows us to look at the J/ψ events in this proposed experiment below the 8.2 GeV production threshold and above. Fig. 15 shows the distribution of the reconstruction photon energies up to 8.5 GeV with SoLID detection resolutions included.

Our main trigger will be a 3-fold coincidence of the decay pair and the recoil proton. There will be some 4-fold electroproduction coincident events including the scattered electrons in the obtained data set for us to study and such a topology shall provide the cleanest signal to background ratio but low statistics. We may choose to include only 2-fold coincident detection of the J/ψ decay pair if the trigger design allows, but it is expected to have large backgrounds for such a topology.

We plan to use beam currents up to 1.25 μA to ensure the luminosity below 1.2×10^{37} nucleon/cm^2/s which is the same as E12-12-006. SoLID collaboration is actively working on improving the J/ψ setup's capability to handle even higher luminosity and we hope to increase the beam current for this experiment accordingly to obtain more statistics.

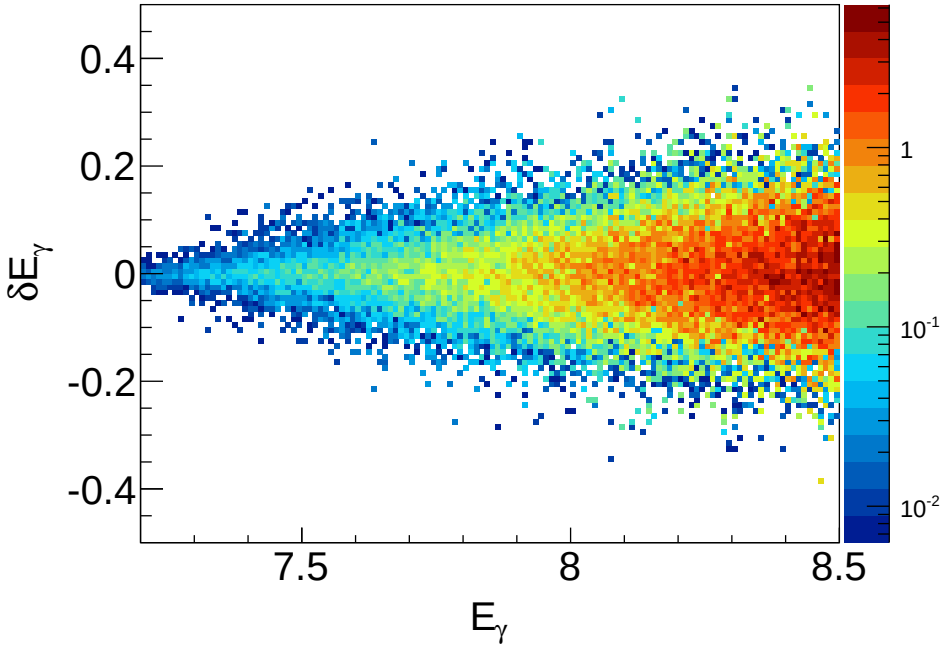

Figure 15: The reconstructed photon energy distribution with SoLID detection resolutions included.

4 Rates and Beam request

4.1 The physics signal

We simulate the J/ψ production channels according to the 5-fold differential cross section grids from the calculation as described in Sec. 2.4. The electron beam energy is set at 8.5 GeV, 300 MeV above the threshold energy of J/ψ production on a free proton. We use a beam current of 1.25 μA and luminosity of 1.2×10^{37} nucleon/cm^2/s for rate estimation. Since we do not require the detection of scattered electrons, the electroproduction and photoproduction events are both simulated. The SoLID acceptance and resolution, as described in Sec. 3, is applied to all final state particles. As protons detected have momentum > 0.2 GeV and there is no neutron detection in SoLID, we do not consider the production of J/ψ from the neutron inside a deuteron in this experiment.

For photoproduction, we first generate a Bremsstruhlung photon, and then the photon interacts with a deuteron to produce the J/ψ. As the subthreshold production cross section decreases fast with decreasing photon energy, we only integrate photons above 7.2 GeV. Apart from the detection of e^+e^- from J/ψ decays, we also require the detection of the recoil proton, which would allow us to reconstruct the relative momentum of the $J/\psi - p$ subsystem and the photon energy as demonstrated in the last section.

Since the intrinsic width of J/ψ is very narrow, the mass spectrum of the e^+e^- from its decay is determined by the detector resolutions, as shown in Fig. 16. The momentum distributions of the positron (or electron) and the recoil proton are shown in Fig. 17. One can observe that the positron (or the electron) only distributes in large angles for subthreshold productions, while the recoil proton has more counts in forward angles. This feature is due to the relatively low momentum of the J/ψ produced below the threshold. In the J/ψ rest frame, the decay e^+e^- are back-to-back. The angle between e^+e^- decreases with J/ψ being boosted to high momenta. In Figs. 18 and 19, we show the momentum distribution of the reconstructed J/ψ and the angle between the decay e^+e^-.

The triple coincident detection of e^+, e^-, and p allows us to track the momentum of J/ψ in the $J/\psi - p$ center-of-mass (c.m.) frame. As demonstrated in Sec. 2.3, the events with lower J/ψ momentum $\kappa_{J/\psi}$ in the $J/\psi - N$ c.m. frame are more sensitive to the $J/\psi - N$ potential. The distribution of $\kappa_{J/\psi}$ is shown in Fig. 20, where the blue curve is the distribution with the proton momentum below 1 GeV, the red curve is the distribution with the proton momentum above 1 GeV, and the black curve is the sum. One can see that the events with higher proton momenta are more likely to have lower $\kappa_{J/\psi}$. In Fig. 21, we show the distributions of $\kappa_{J/\psi}$ versus the momentum and the polar angle of the proton.

For electroproduction, the virtual photon flux is calculated by applying the one-photon-exchange approximation. Since we do not require the detection of the scattered electron, it is generated in the full phase space. Similar to the photoproduction case, the mass spectrum

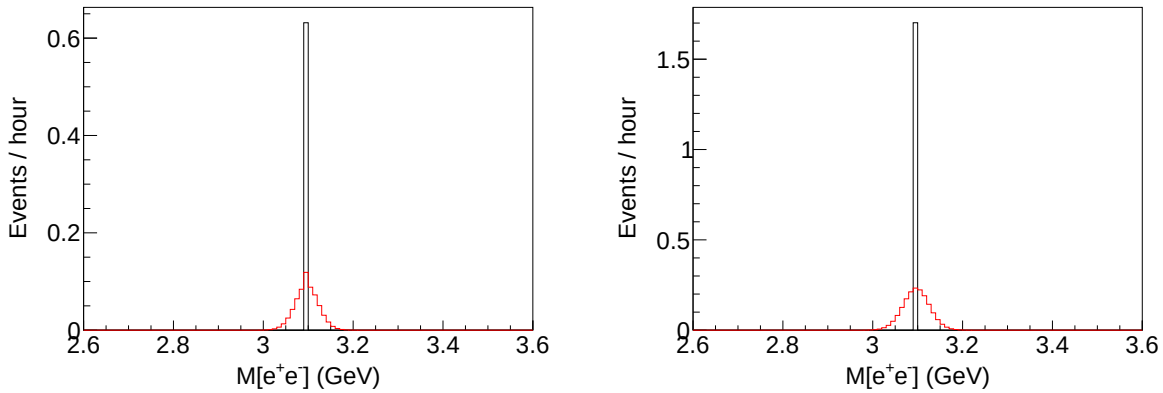

Figure 16: The spectrum of the e^+e^- from the photoproduction of J/ψ below the threshold (left) and above the threshold (right). The black curves are before the smearing with detector resolutions, and the red curves are after the smearing.

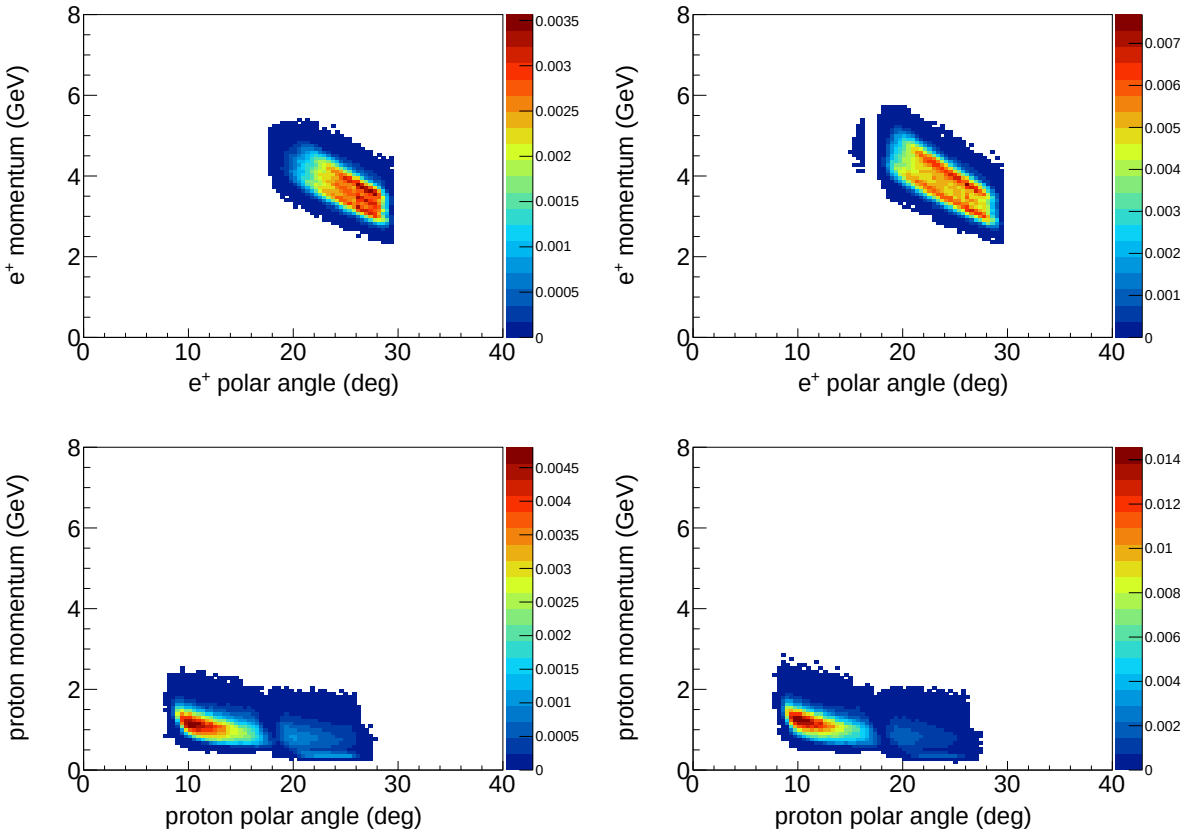

Figure 17: The momentum distributions of the detected e^+ and proton with the photoproduction of J/ψ below the threshold (left) and above the threshold (right).

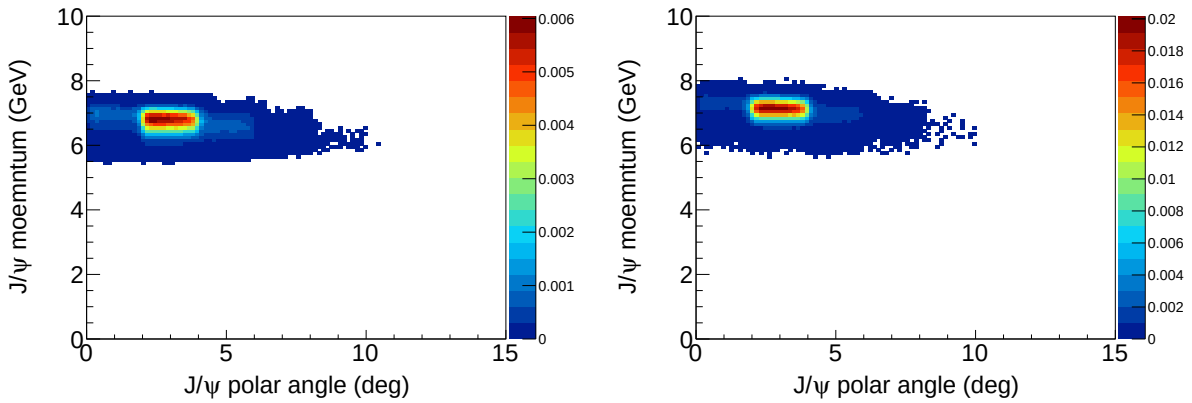

Figure 18: The momentum distribution of reconstructed J/ψ from photoproduction below the threshold (left) and above the threshold (right).

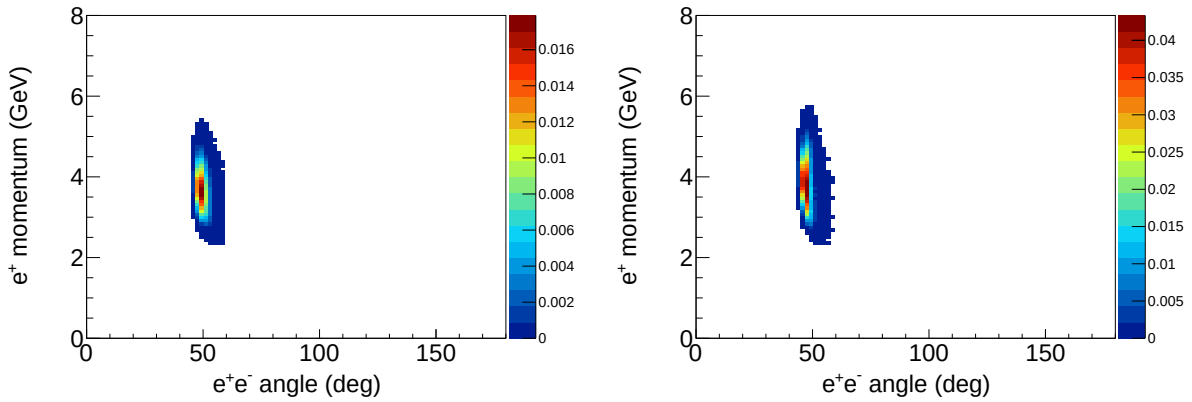

Figure 19: The angle between the decay e^+e^- from J/ψ photoproduction below the threshold (left) and above the threshold (right).

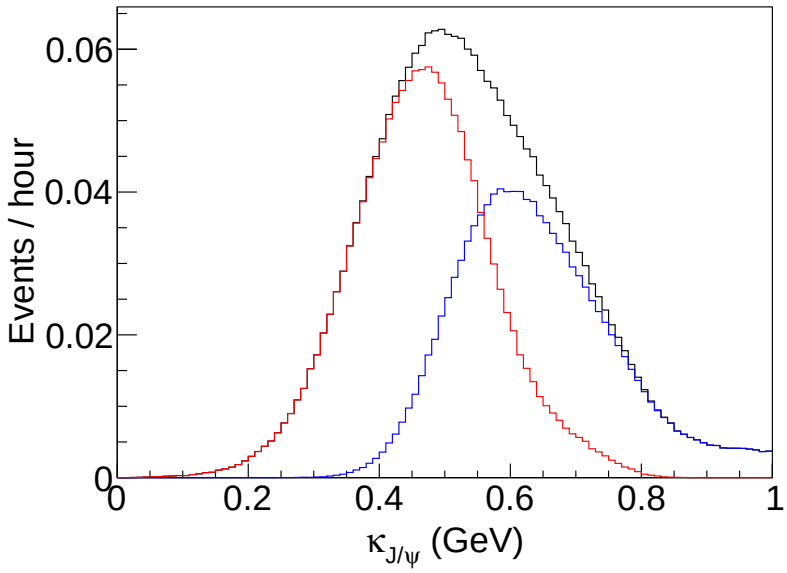

Figure 20: The momentum of J/ψ (from the photoproduction) in the $J/\psi - p$ c.m. frame. The blue curve is the distribution with the proton momentum in the lab frame below 1 GeV, the red curve is the distribution with the proton momentum above 1 GeV, and the black curve is the sum.

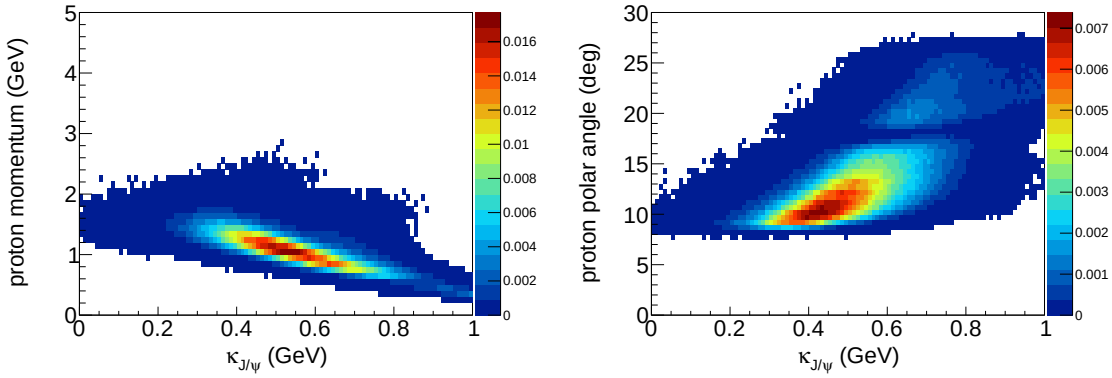

Figure 21: The distributions of J/ψ (from the photoproduction) momentum in the $J/\psi - p$ c.m. frame versus the proton momentum (left) and the proton polar angle.

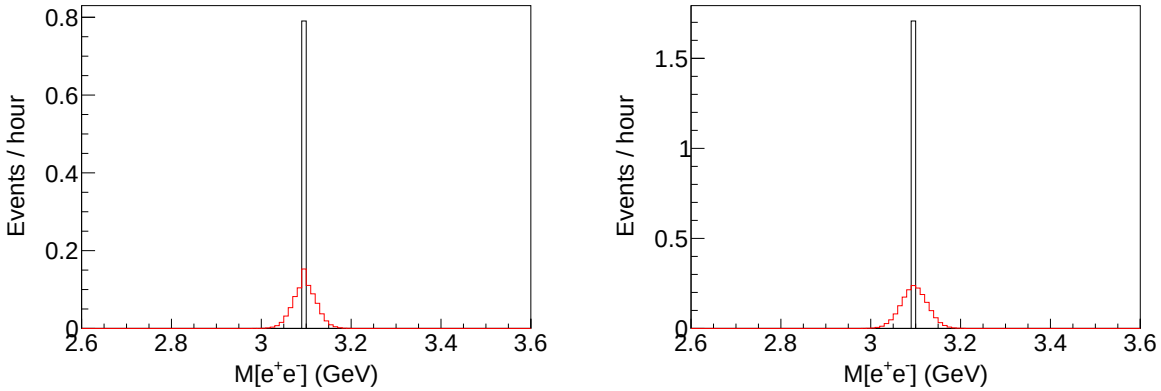

Figure 22: The spectrum of the e^+e^- from the electroproduction of J/ψ with the virtual photon energy below the threshold (left) and above the threshold (right). The black curves are before the smearing, and the red curves are after the smearing.

of the decay e^+e^- is shown in Fig. 22, and the momentum distributions of the detected positron (or electron) and the proton are shown in Fig. 23. The momentum distributions of the reconstructed J/ψ are shown in Fig. 24, and the angle between the positron and the electron are shown in Fig. 25. The distributions of J/ψ momentum in the $J/\psi - p$ c.m. frame are shown in Figs. 26 and 27.

The event rate of J/ψ production below the threshold and above the threshold can be read off from Fig. 16 for the photoproduction and from Fig. 22 for the electroproduction. For a more realistic estimation, we assume an overall detection efficiency factor of 0.8 in addition to the SoLID acceptance that has been applied in Figs. 16-27. Without cut on the J/ψ invaraint mass, the J/ψ photoproduction rate is 0.51/hour below the threshold and 1.36/hour above the threshold. The electroproduction rate is 0.63/hour below the threshold and 1.37/hour above the threshold. The total event counts for 47 days are 2106 for the photoproduction and 2254 for the electroproduction. In the aforementioned 3-fold coincident detection, the photoproduction and the electroproduction can not be separated from each other, as the scattered electron is not required to be detected. So the measured event counts are the sum of the photoproduction and the electroproduction, *i.e.* 1.14/hour and 1283 for 47 days below the threshold, and 2.73/hour and 3077 for 47 days above the threshold. A projection as a function of the J/ψ momentum in the c.m. frame of the J/ψ and the proton ($\kappa_{J/\psi}$) with the recoil proton momentum above 1 GeV is shown in Fig. 28. The low momentum region of $\kappa_{J/\psi}$ is sensitive to the $J/\Psi - N$ potential [20]. A projection as a function of the reconstructed photon energy E_γ with the recoil proton momentum above 1 GeV is shown in Fig. 29.

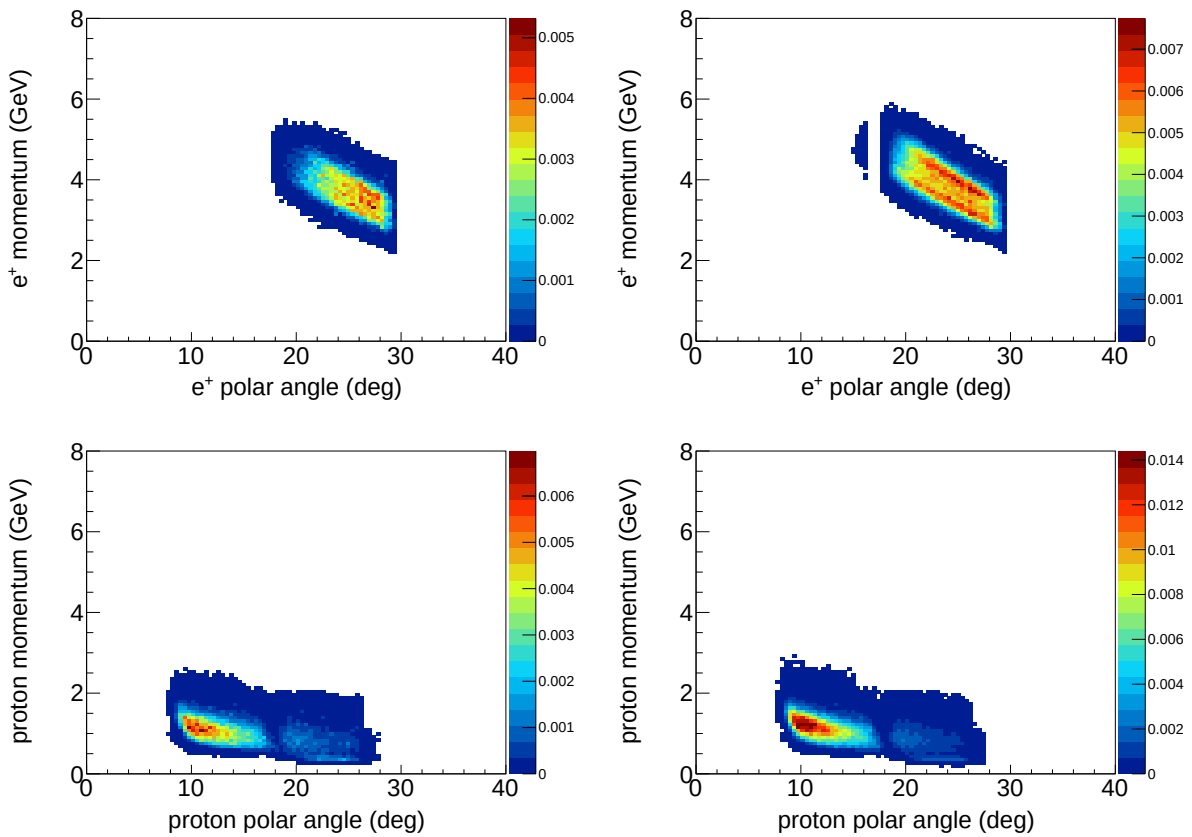

Figure 23: The momentum distributions of the detected e^+ and proton from the electroproduction of J/ψ with the virtual photon energy below the threshold (left) and above the threshold (right).

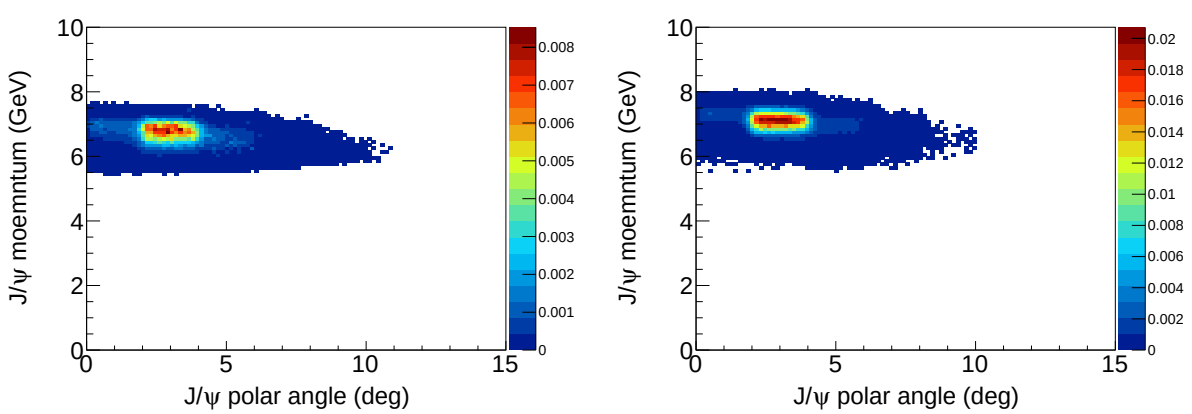

Figure 24: The momentum distribution of reconstructed J/ψ from the electroproduction with the virtual photon energy below the threshold (left) and above the threshold (right).

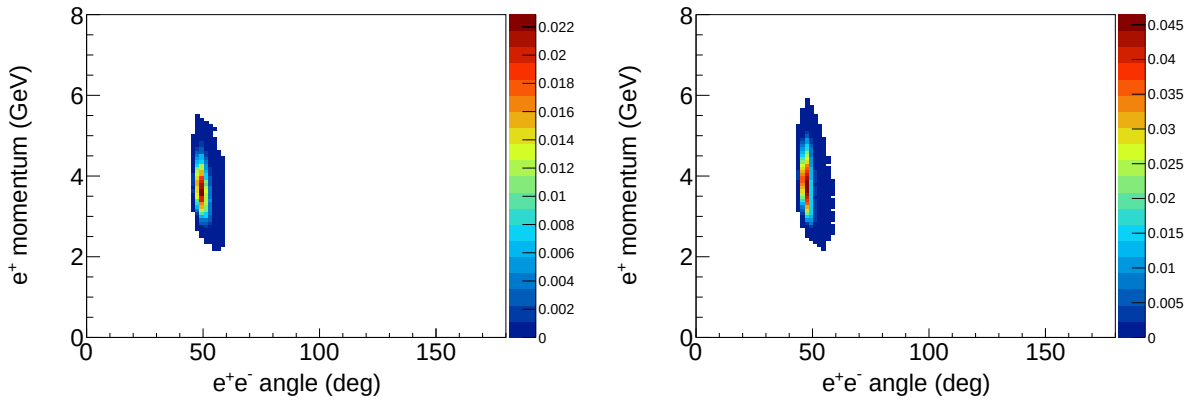

Figure 25: The angle between the decay e^+e^- from J/ψ electroproduction with the virtual photon energy below the threshold (left) and above the threshold (right).

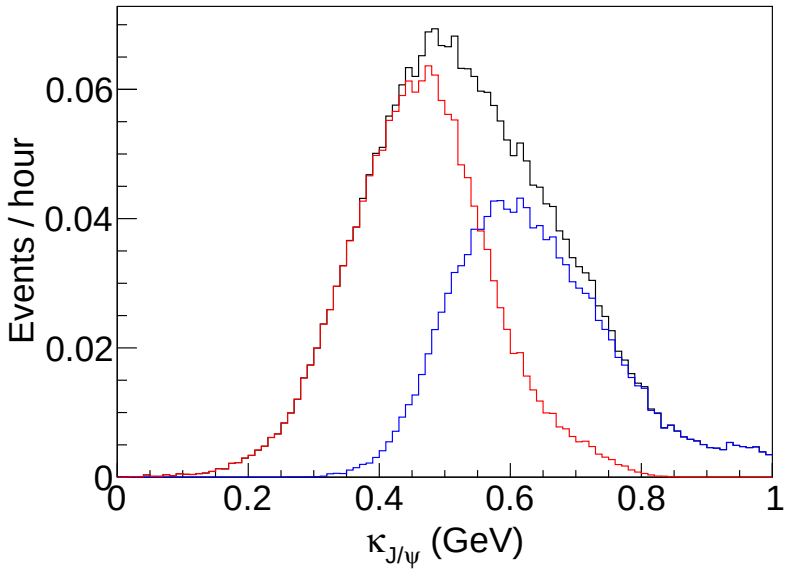

Figure 26: The momentum of J/ψ (from the electroproduction) in the $J/\psi - p$ c.m. frame. The blue curve is the distribution with the proton momentum in the lab frame below 1 GeV, the red curve is the distribution with the proton momentum above 1 GeV, and the black curve is the sum.

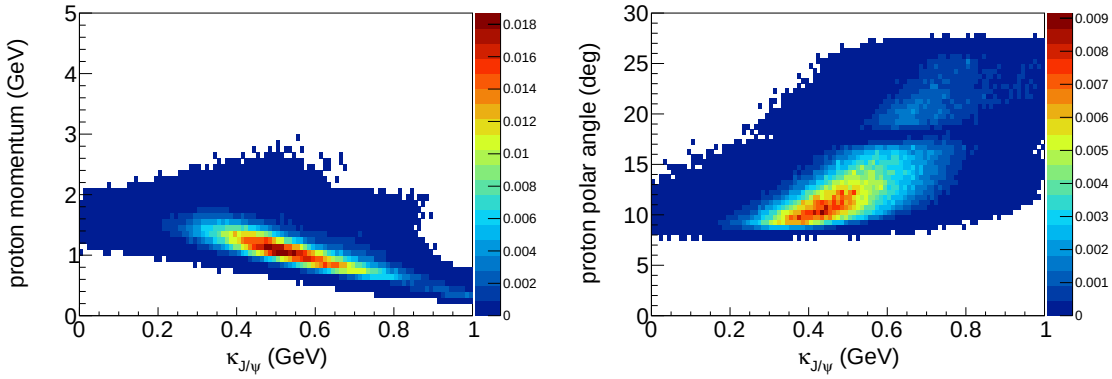

Figure 27: The distributions of J/ψ (from the electroproduction) momentum in the $J/\psi - p$ c.m. frame versus the proton momentum (left) and the proton polar angle (right).

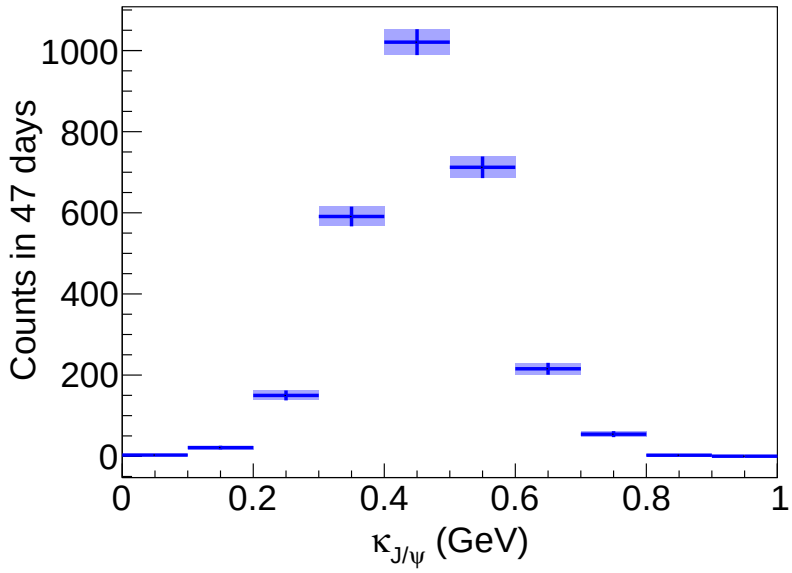

Figure 28: The projected J/ψ counts for 47 days of beam on target from the sum of photoproduction and electroproduction with the recoil proton momentum above 1 GeV, corresponding to the low $\kappa_{J/\psi}$ region as illustrated in Figs. 20 and 26. An overall detector efficiency factor 0.8 is included. The vertical width of the filled bands is the statistical uncertainty, while the horizontal width indicates the bin size.

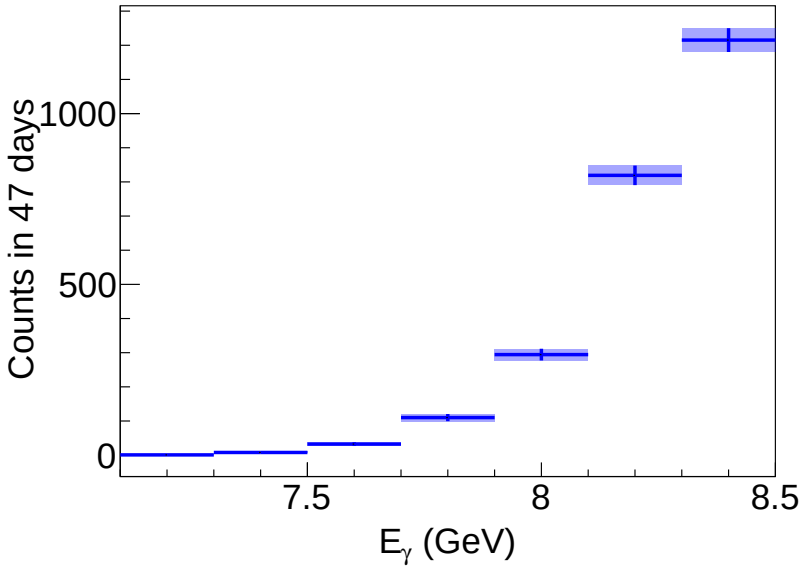

Figure 29: The projected J/ψ counts as a function of the reconstructed photon energy for 47 days of beam on target from the sum of photoproduction and electroproduction with the recoil proton momentum above 1 GeV, corresponding to the low $\kappa_{J/\psi}$ region as illustrated in Figs. 20 and 26. An overall detector efficiency factor 0.8 is included. The vertical width of the filled bands is the statistical uncertainty, while the horizontal width indicates the bin size.

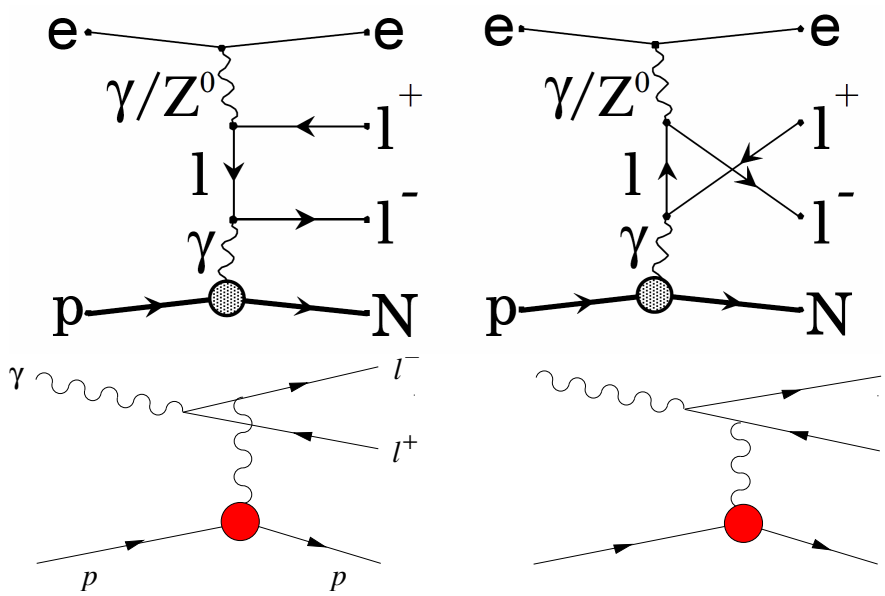

Figure 30: Two-photon Bethe-Heitler process with dilepton in final state with an electron beam (top) or photon beam (bottom).

4.2 The backgrounds

Pythia program was used to investigate if there is any physics background near the J/ψ production threshold from the proton and at the JLab kinematics region. And there is no physics background found, mainly due to the large mass of J/ψ meson [12]. The only expected physics background is the well known two-photon Bethe-Heitler (BH) process shown in Fig. 30. It consists of the same final state particles as the J/ψ production and decay. The resulting electron and positron from the BH process can have an invariant mass at 3.1 GeV, thus can not be distinguished from J/ψ.

In order to evaluate this background rate at our kinematics, we simulated BH events from quasi-real photons of electron scattering, according to the equivalent photon approximation (EPA), and real photons from Bremsstrahlung on the target. The cross section was calculated from the QED Feynman diagrams [55] and the off-shell proton in a deuteron was simulated with its momentum distribution. We used the same beam and target conditions of the J/ψ simulation and also applied the same SoLID acceptance and resolutions to have a meaningful comparison. Finally the same overall detector efficiency 80% is also applied. The expected background events from the BH process are shown in Fig. 31. We choose a cut of 120 MeV width around 3.1 GeV to collect 98% of J/ψ events and then use the same width to obtain the background BH event rate of 0.277 (0.272) counts/hour from photoproduction below (above) the threshold, and 0.543 (0.441) counts/hour from electroproduction below (above) the threshold.

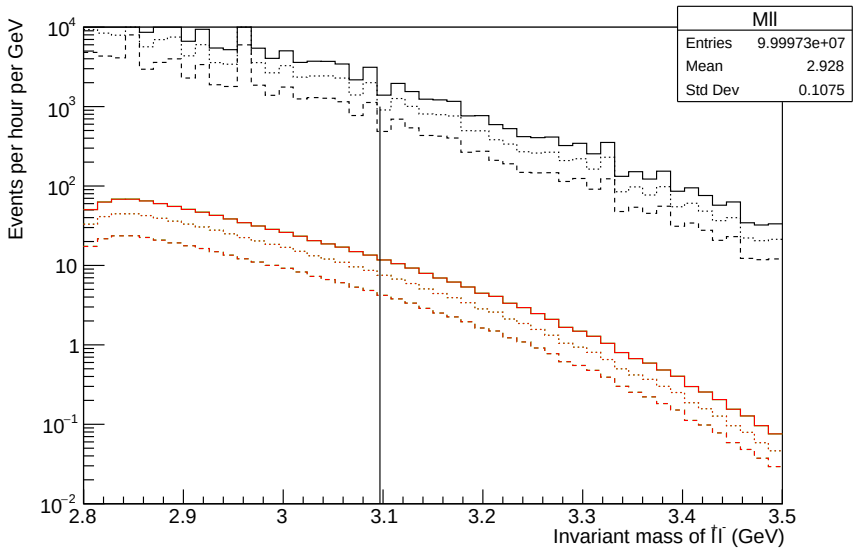

Figure 31: BH process event rates. The dotted line is from electroproduction, dashed line is from photoproduction, and solid line includes both. Color black stands for all generated events and color red is for events detected by SoLID with momentum smearing according to its resolution.

In this LOI the proposed target will be a liquid deuterium target, so we will need to consider additional backgrounds such as the initial J/Ψ production is on the neutron inside the deuteron, which then can be followed by a charge-exchange process leading to the same final state as that of the signal channel. While we do plan to carry out a detailed simulation of such a two-step process during the proposal stage, this background channel is expected to be suppressed. We have carried out a study of another possible background channel, which is $\gamma +$ "p" $\rightarrow p + J/\psi + \pi^0$, where "$p$" stands for the proton inside the deuteron. While the kinematic phase space for this channel overlaps with that of the signal channel, namely the $\gamma +$ "p" $\rightarrow J/\psi + p$, the cross section for this three-particle final state channel is expected to be highly suppressed, especially in the subthreshold region. At the proposal stage, we will carry out studies of any additional possible background channels.

4.3 Beam request

In this experiment, we propose to measure the J/ψ subthreshhold production cross section on a 15-cm long liquid deuterium target at SoLID. The beam energy required is 8.5 GeV and beam current is 1.25 μA. This corresponds to a luminosity of 1.2×10^{37} nucleon/cm^2/s, which is the same as the approved SoLID J/ψ experiment (E12-12-006) on a liquid hydrogen target. Taking into account the SoLID acceptance, detector resolutions, an overall detection

efficiency of 80%, and a 120 MeV wide J/ψ mass cut, we show both the signal and background rates in Table 1 for sub- and near-threshold kinematics. We request 50 days of beam time including 47 days for production data taking and 3 days for dedicated aluminum dummy runs and detector studies. Data from aluminum dummy runs will be used for subtracting backgrounds from the target windows, and additional detector studies beyond E12-12-006 might also be needed. We will obtain a total number of 1262 subthreshhold J/ψ events on top of 925 BH background events and 2982 above-the-threshold J/ψ events on top of 804 BH background events.

This beam request is based on Harry Lee's calculation using a Pomeron-exchange model. His recent Pomeron-LQCD model [28] predicts the total J/ψ photoproduction cross section from the nucleon that is up to one order of magnitude larger compared to that from the Pomeron-exchange model. We very much look forward to the new results from the Hall C experiment (E12-16-007) on the J/ψ photoproduction cross section from the proton which will provide additional tests of the Pomeron-LQCD model prediction in addition to the GlueX results [4]. So the signal rates used in this proposed experiment are conservative. If the rates are indeed significantly higher than those used in this LOI, the experiment could achieve significantly better statistics with the same amount of beam time, that is crucial for the low $\kappa_{J/\psi}$ region as shown in Fig. 28. Further, if the overall data taking rate can be improved by the time SoLID is running, this proposed experiment could run at a much higher beam current, which would help again with the statistics of the experiment, and possibly also allow for a reduction of the required beam time. For the future development of a full proposal, we plan to incorporate the theoretical calculations into our Monte Carlo simulation of the experiment, and to quantify the impact of the proposed measurements concerning both the $J/\psi - N$ interaction and also the SRC effect.

Table 1: The event counts of e^+e^- within the 120 MeV cut around J/ψ mass for 47 days of a 8.5 GeV and 1.25 uA electron beam on a 15 cm LD_2 target.

Channel	J/ψ below threshold	J/ψ above threshold	BH below threshold	BH above threshold
Photoproduction	560	1487	312	307
Electroproduction	702	1495	613	497
Total	1262	2982	925	804

5 Summary

In this letter of intent, we propose to carry out a first measurement of both sub- and near-threshold electro- and photo-production of J/ψ mesons from a 15-cm liquid deuterium target using the proposed SoLID apparatus in Hall A with an electron beam at 8.5 GeV and a beam current of 1.25 μA. The requested beam time is 50 days with 47 days for

production data taking on LD_2 target and 3 days dedicated for aluminum dummy runs and some detector studies, which will lead to a total sub-threshold J/ψ events of more than 1250, and nearly 3000 near the threshold based on rather conservative estimations of the rates (see Section 4.3). The proposed experiment will be the first to demonstrate sub-threshold production of J/ψ and to show sensitivity – using the state-of-the-arts calculations – to the $J/\psi - N$ interaction and test the lattice QCD prediction. The data will reveal the short-range correlation in deuteron for determining the short-range part of nucleon-nucleon potentials used in the state-of-the-art nuclear many-body calculations. This is an important first step towards testing the universality of the nucleon-nucleon short-range correlations in nuclear scattering processes, which is necessary for SRC to be the origin of the EMC effect by proposing future sub-threshold production of J/ψ from other nuclear targets such as ^{12}C and ^{4}He.

References

[1] M. Gell-Mann, Phys. Lett. **8**, 214 (1964).

[2] R. Aaij et al. (LHCb Collaboration), Phys. Rev. Lett. **115**, 072001 (2015).

[3] R. Aaij et al. (LHCb Collaboration), arXiv: **1904.03947** (2019).

[4] A. Ali, M. Amaryan, E. G. Anassontzis, A. Austregesilo, M. Baalouch, F. Barbosa, J. Barlow, A. Barnes, E. Barriga, T. D. Beattie, et al. (GlueX Collaboration), Phys. Rev. Lett. **123**, 072001 (2019), URL https://link.aps.org/doi/10.1103/PhysRevLett.123.072001.

[5] S. Brodsky, E. Chudakov, P. Hoyer, and J. Laget, Physics Letters B **498**, 23 (2001), ISSN 0370-2693, URL http://www.sciencedirect.com/science/article/pii/S0370269300013733.

[6] S. Joosten, Z.-E. Meziani, M. Paolone, E. Chudakov, and M. Jones, Jefferson Lab Experiment E12-16-007 (2016), URL http://www.jlab.org/exp_prog/proposals/16/PR12-16-007.pdf.

[7] X.-D. Ji, Phys. Rev. Lett. **74**, 1071 (1995).

[8] X. Ji, Phys. Rev. D **52**, 271 (1995), URL https://link.aps.org/doi/10.1103/PhysRevD.52.271.

[9] D. Kharzeev, Proc. Int. Sch. Phys. Fermi **130**, 105 (1996), nucl-th/9601029.

[10] D. Kharzeev, H. Satz, A. Syamtomov, and G. Zinovjev, Eur. Phys. J. C **9**, 459 (1999), URL https://doi.org/10.1007/s100520050039.

[11] A. Deur, S. Brodsky, and G. de Téramond, Physics Letters B **750**, 528 (2015), ISSN 0370-2693, URL http://www.sciencedirect.com/science/article/pii/S0370269315007388.

[12] K. Hafidi, Z.-E. Meziani, N. Sparveris, X. Qian, and Z. W. Zhao, Jefferson Lab Experiment E12-12-006 (2012), URL http://www.jlab.org/exp_prog/proposals/12/PR12-12-006.pdf.

[13] M. E. Peskin, Nuclear Physics B **156**, 365 (1979), ISSN 0550-3213, URL http://www.sciencedirect.com/science/article/pii/0550321379901998.

[14] M. Luke, A. V. Manohar, and M. J. Savage, Physics Letters B **288**, 355 (1992), ISSN 0370-2693, URL http://www.sciencedirect.com/science/article/pii/0370269392911140.

[15] S. J. Brodsky and G. A. Miller, Physics Letters B **412**, 125 (1997), ISSN 0370-2693, URL http://www.sciencedirect.com/science/article/pii/S0370269397010459.

[16] A. B. Kaidalov and P. E. Volkovitsky, Phys. Rev. Lett. **69**, 3155 (1992), URL https://link.aps.org/doi/10.1103/PhysRevLett.69.3155.

[17] T. Kawanai and S. Sasaki, Phys. Rev. D **82**, 091501 (2010), URL https://link.aps.org/doi/10.1103/PhysRevD.82.091501.

[18] S. J. Brodsky, I. Schmidt, and G. F. de Téramond, Phys. Rev. Lett. **64**, 1011 (1990), URL https://link.aps.org/doi/10.1103/PhysRevLett.64.1011.

[19] J.-J. Wu and T.-S. H. Lee, Phys. Rev. C **86**, 065203 (2012), URL https://link.aps.org/doi/10.1103/PhysRevC.86.065203.

[20] J.-J. Wu and T.-S. H. Lee, Phys. Rev. C **88**, 015205 (2013), URL https://link.aps.org/doi/10.1103/PhysRevC.88.015205.

[21] X. Qian, W. Chen, H. Gao, K. Hicks, K. Kramer, J. Laget, T. Mibe, Y. Qiang, S. Stepanyan, D. Tedeschi, et al., Physics Letters B **696**, 338 (2011), ISSN 0370-2693, URL http://www.sciencedirect.com/science/article/pii/S0370269311000037.

[22] P. Bosted, J. Dunne, C. A. Lee, P. Junnarkar, M. Strikman, J. Arrington, R. Asaturyan, F. Benmokhtar, M. E. Christy, E. Chudakov, et al., Phys. Rev. C **79**, 015209 (2009), URL https://link.aps.org/doi/10.1103/PhysRevC.79.015209.

[23] Y. Hatta, M. Strikman, J. Xu, and F. Yuan, Physics Letters B **803**, 135321 (2020), ISSN 0370-2693, URL http://dx.doi.org/10.1016/j.physletb.2020.135321.

[24] P. Bosted and E. Chudakov, Jefferson Lab Proposal PR12-07-106 (2007), URL http://www.jlab.org/exp_prog/proposals/07/PR12-07-106.pdf.

[25] Y. Ilieva, B. McKinnon, P. Nadel-Turonski, V. Kubarovsky, S. Stepanyan, and Z. W. Zhao, Jefferson Lab Experiment E12-11-003b (2018), URL https://www.jlab.org/exp_prog/proposals/18/E12-11-003B.pdf.

[26] K. Yokokawa, S. Sasaki, T. Hatsuda, and A. Hayashigaki, Phys. Rev. D **74**, 034504 (2006), URL https://link.aps.org/doi/10.1103/PhysRevD.74.034504.

[27] N. Ishii, S. Aoki, and T. Hatsuda, Phys. Rev. Lett. **99**, 022001 (2007), URL https://link.aps.org/doi/10.1103/PhysRevLett.99.022001.

[28] T. S. H. Lee, arXiv:2004.13934 (2020), URL https://arxiv.org/abs/2004.13934.

[29] L. Frankfurt, M. Sargsian, and M. Strikman, International Journal of Modern Physics A **23**, 2991 (2008), URL https://doi.org/10.1142/S0217751X08041207.

[30] J. Arrington, D. Higinbotham, G. Rosner, and M. Sargsian, Progress in Particle and Nuclear Physics **67**, 898 (2012), ISSN 0146-6410, URL http://www.sciencedirect.com/science/article/pii/S0146641012000749.

[31] O. Hen, D. W. Higinbotham, G. A. Miller, P. Eli, and L. B. Weinstein, International Journal of Modern Physics E **22**, 1330017 (2013), URL https://doi.org/10.1142/S0218301313300178.

[32] O. Hen, G. A. Miller, E. Piasetzky, and L. B. Weinstein, Rev. Mod. Phys. **89**, 045002 (2017), URL https://link.aps.org/doi/10.1103/RevModPhys.89.045002.

[33] N. Fomin, D. Higinbotham, M. Sargsian, and P. Solvignon, Annual Review of Nuclear and Particle Science **67**, 129 (2017), URL https://doi.org/10.1146/annurev-nucl-102115-044939.

[34] I. C. Cloët, R. Dupré, S. Riordan, W. Armstrong, J. Arrington, W. Cosyn, N. Fomin, A. Freese, S. Fucini, D. Gaskell, et al., Journal of Physics G: Nuclear and Particle Physics **46**, 093001 (2019), ISSN 1361-6471, URL http://dx.doi.org/10.1088/1361-6471/ab2731.

[35] K. S. Egiyan, N. B. Dashyan, M. M. Sargsian, M. I. Strikman, L. B. Weinstein, G. Adams, P. Ambrozewicz, M. Anghinolfi, B. Asavapibhop, G. Asryan, et al. (CLAS Collaboration), Phys. Rev. Lett. **96**, 082501 (2006), URL https://link.aps.org/doi/10.1103/PhysRevLett.96.082501.

[36] J. Seely, A. Daniel, D. Gaskell, J. Arrington, N. Fomin, P. Solvignon, R. Asaturyan, F. Benmokhtar, W. Boeglin, B. Boillat, et al., Phys. Rev. Lett. **103**, 202301 (2009), URL https://link.aps.org/doi/10.1103/PhysRevLett.103.202301.

[37] L. B. Weinstein, E. Piasetzky, D. W. Higinbotham, J. Gomez, O. Hen, and R. Shneor, Phys. Rev. Lett. **106**, 052301 (2011), URL https://link.aps.org/doi/10.1103/PhysRevLett.106.052301.

[38] N. Fomin, J. Arrington, R. Asaturyan, F. Benmokhtar, W. Boeglin, P. Bosted, A. Bruell, M. H. S. Bukhari, M. E. Christy, E. Chudakov, et al., Phys. Rev. Lett. **108**, 092502 (2012), URL https://link.aps.org/doi/10.1103/PhysRevLett.108.092502.

[39] O. Hen, E. Piasetzky, and L. B. Weinstein, Phys. Rev. C **85**, 047301 (2012), URL https://link.aps.org/doi/10.1103/PhysRevC.85.047301.

[40] J. Arrington, A. Daniel, D. B. Day, N. Fomin, D. Gaskell, and P. Solvignon, Phys. Rev. C **86**, 065204 (2012), URL https://link.aps.org/doi/10.1103/PhysRevC.86.065204.

[41] O. Hen, M. Sargsian, L. B. Weinstein, E. Piasetzky, H. Hakobyan, D. W. Higinbotham, M. Braverman, W. K. Brooks, S. Gilad, K. P. Adhikari, et al., Science **346**, 614 (2014), ISSN 0036-8075, URL https://science.sciencemag.org/content/346/6209/614.

[42] E. O. Cohen, O. Hen, E. Piasetzky, L. B. Weinstein, M. Duer, A. Schmidt, I. Korover, H. Hakobyan, S. Adhikari, Z. Akbar, et al. (CLAS Collaboration), Phys. Rev. Lett. **121**, 092501 (2018), URL https://link.aps.org/doi/10.1103/PhysRevLett.121.092501.

[43] L. Weinstein, S. Bültmann, D. Bulumulla, G. Charles, G. Dodge, F. Hauenstein, C. Hyde, A. Klein, S. Nadeeshani, Y. Prok, et al., Nature **560** (2018), URL https://www.nature.com/articles/s41586-018-0400-z.

[44] M. Duer, A. Schmidt, J. R. Pybus, E. P. Segarra, A. Hrnjic, A. W. Denniston, R. Weiss, O. Hen, E. Piasetzky, L. B. Weinstein, et al. (CLAS Collaboration), Phys. Rev. Lett. **122**, 172502 (2019), URL https://link.aps.org/doi/10.1103/PhysRevLett.122.172502.

[45] B. Schmookler et al., Nature **566**, 354 (2019), URL https://doi:10.1038/s41586-019-0925-9.

[46] M. A. Pichowsky and T.-S. H. Lee, Phys. Rev. D **56**, 1644 (1997), URL https://link.aps.org/doi/10.1103/PhysRevD.56.1644.

[47] C. D. Roberts, private communications.

[48] R. B. Wiringa, V. G. J. Stoks, and R. Schiavilla, Phys. Rev. C **51**, 38 (1995), URL https://link.aps.org/doi/10.1103/PhysRevC.51.38.

[49] M. Piarulli and I. Tews, Frontiers in Physics **7**, 245 (2020), ISSN 2296-424X, URL https://www.frontiersin.org/article/10.3389/fphy.2019.00245.

[50] M. Derrick et al. (ZEUS), Phys. Lett. B **350**, 120 (1995), hep-ex/9503015.

[51] S. Aid et al. (H1), Nucl. Phys. B **468**, 3 (1996), [Erratum: Nucl.Phys.B 548, 639–639 (1999)], hep-ex/9602007.

[52] B. Gittelman, K. Hanson, D. Larson, E. Loh, A. Silverman, and G. Theodosiou, Phys. Rev. Lett. **35**, 1616 (1975).

[53] U. Camerini, J. Learned, R. Prepost, C. M. Spencer, D. Wiser, W. Ash, R. L. Anderson, D. Ritson, D. Sherden, and C. K. Sinclair, Phys. Rev. Lett. **35**, 483 (1975).

[54] A. Donnachie and P. Landshoff, Nuclear Physics B **244**, 322 (1984), ISSN 0550-3213, URL http://www.sciencedirect.com/science/article/pii/0550321384903158.

[55] M. Diehl, M. Diehl, and B. Pire, European Physical Journal C - Particles and Fields **23**, 675 (2002), URL https://link.springer.com/article/10.1007/s100520200917.